1-1-2010

The Roles Of Rhle And Hfq In Srna-Dependent Gene Regulation

Abeykoon Jayalath Iresha Sandeepanie Rathnayake
Wayne State University

THE ROLES RHLE AND HFQ IN sRNA-DEPENDENT GENE REGULATION

by

ABEYKOON JAYALATH IRESHA SANDEEPANIE RATHNAYAKE

THESIS

Submitted to the Graduate School

of Wayne State University,

Detroit, Michigan

in partial fulfillment of the requirements

for the degree of

MASTER OF SCIENCE

2010

MAJOR: CHEMISTRY

Approved by:

_____

Advisor Date

_____

_____

DEDICATION

This thesis is dedicated to my parents

ACKNOWLEDGEMENTS

I would like to express my sincere gratitude to my advisor Dr. Andrew Feig for his support, guidance and patience in this accomplishment.

I would also like to thank my committee members Dr. Tamara Hendrickson and Dr. Mary K. Pflum for their support.

I would like to express my appreciation to all my lab members for their help and wonderful friendship.

TABLE OF CONTENTS

LIST OF TABLES

LIST OF FIGURES

CHAPTER ONE

INTRODUCTION

Significance

Bacterial infectious diseases cause a significant number of deaths worldwide every year. In the past few years, several studies discovered that small non-coding RNAs (sRNAs) play an emerging role in modulation of bacterial pathogenesis and virulence (1-4). RNAIII came into picture as the first RNA regulator in pathogenesis of bacteria. RNAIII regulates multiple targets in *Staphylococcus aureus* including *SA-1000* mRNA, which encodes a protein involved in adherence and invasion of host cells (5,6). Padalon-Brauch et al. in 2008 identified 19 novel sRNAs encoded within pathogenecity islands of *Salmonella typhimurium* and observed that these sRNAs showed induced expression levels in the stage of infection allowing adaptation of *Salmonella* to extreme acidic environment of the stomach. *Vibrio cholerae* has multiple sRNAs which ensure efficient colonization in the human intestine (7). In contrast, a recent study has identified vrrA sRNA as a negative regulator of *Vibrio cholerae* pathogenecity (2). Nevertheless, it has been found that numerous other infectious bacterial species including *Listeria monocytogenes*, *Pseudomonas aeruginosa* and *Chlamydia trachomatis* show sRNA dependent virulence (2,3). The importance of sRNA-mediated gene regulation for the virulence and pathogenecity of bacteria highlights that these regulation processes can be potential targets for the successful eradication of pathogenic bacteria. Thus, it is

necessary to understand bacterial sRNA-mediated regulatory processes and the protein components that are associated with sRNAs, to exploit these pathways for new anti-infectives.

Roles of sRNAs in gene regulation

Bacteria are adapted to live in diverse environmental conditions. Thus, they show excellent tolerance and response to extreme environmental conditions caused by low or high temperatures, high salinity, reactive oxygen species or high nutrient concentrations. The adaptation is acquired by gene acquisition, gene mutation or the regulation of gene expression (8-10).

Gene expression regulation is performed at different levels and is governed by different factors. While protein regulators function at any level of the pathway, RNA regulators specifically act at transcriptional or post-transcriptional levels. At the post-transcriptional level they activate or deactivate the translation of a particular mRNA (11,12).

Being a part of the 5' untranslated region (UTR) region of the mRNA sequence that they regulate, riboswitches can be considered as the simplest form of cis-acting RNA regulation (13). Riboswitches undergo structural changes upon binding the small metabolite ligands, such as flavin mononucleotide (FMN), thiamin pyrophosphate (TPP) or S-adenosylmethionine and can act as a part of negative or positive feedback loops. For example, the glmS riboswitch, upon binding its ligand glucosamine-6-phosphate, acts as a ribozyme to cleave itself

and inactivates *glmS* mRNA that codes for the glucosamine-6-phosphate synthase (13,14). The conformational changes include formation of hairpin structures that block or release the ribosome binding site (RBS) or act as transcriptional terminators or anti-terminators (Figure 1 A).

The largest class of RNA regulators consists of cis-encoded or trans-encoded sRNAs. Cis-encoded RNAs are transcribed from the same locus as the gene they regulate and have perfect base complementarity to their target. On the other hand trans-encoded RNAs are transcribed from a separate locus than their target gene and have imperfect base-pairing. This imperfect base-pairing allows some trans-encoded RNAs to regulate multiple targets which creates a web of regulation in the cell (11-13,15).

MicF was identified as the first small RNA regulator that controls gene expression by an anti-sense mechanism in bacteria. It base-pairs with ompF mRNA and represses the synthesis of an outer membrane porin, OmpF. Since then, a significant number of sRNAs have been identified and characterized as post-transcriptional regulators in diverse cellular processes including virulence and adaptation to environmental stress (12,13,15,16).

Interactions of sRNAs and target mRNAs result in translational repression, translational activation or/and degradation of the target (Figure 1B). The majority of regulatory small RNAs found in *E.coli* require the RNA binding protein Hfq to perform their roles in gene regulation (11,13,15-17).

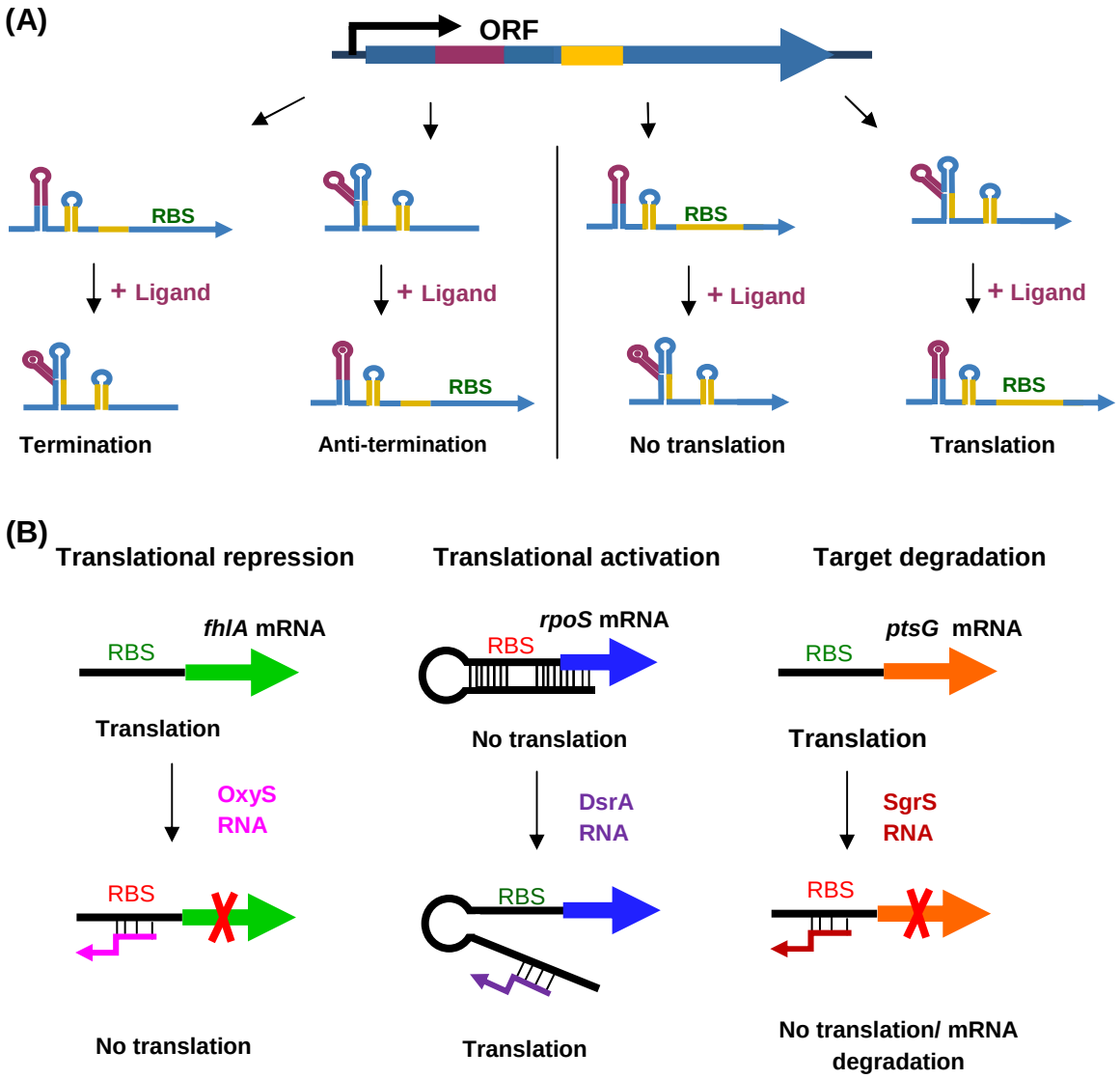

Figure 1: Mechanisms of RNA-mediated gene regulation. **(A)** Riboswitch-mediated regulation. Riboswitches have two main regulatory regions; aptamer region (pink) and expression (yellow) platform. Upon binding the ligand to the aptamer region, the expression platform undergoes structural changes that act as transcriptional terminators or anti-terminators (Left) or block or release ribosome binding site (Right) (13). **(B)** Regulatory outcomes brought by sRNA-mRNA interactions. Bacterial sRNAs are involved in translational repression, activation or/and target degradation (18,19).

Role of Hfq in post-transcriptional gene expression regulation

Hfq was initially identified as a host factor required for Qβ RNA bacteriophage replication (20). Several studies have shown that Hfq plays a prominent role as a post-transcriptional regulator by facilitating the base-pairng between sRNA and mRNA (11,20,21). Its structural homology led it to be categorized as a member of the Sm/Lsm protein family (20). Eukaryotic Sm and Lsm proteins are heterohexamers and are involved in RNA metabolism including mRNA splicing (22). In contrast, Hfq is a homohexameric protein containing 6 copies of an 11 kDa polypeptide forming a heat stable, doughnut shaped structure (4,20). It binds to sRNAs and target mRNAs and shows similar RNA binding specificities to Sm/Lsm proteins (4,20,22,23).

Bacteria containing Hfq mutations show decreased growth rates, increased sensitivity to stress conditions, reduced virulence and irregular cell shapes indicating the importance of this global regulator for the fitness of the bacterial cell (24). Recent studies showed that Hfq is essential for virulence and environmental adaptation of many pathogenic bacteria (25-27). Hfq plays an important role in *Salmonella typimurium* gene regulation by interacting with nearly 50% of sRNAs and 20% of mRNAs including mRNAs that code for pathogenicity islands (25,27). Furthermore, it has been found that Hfq is a critical component of colonization for uropathogenic *E. coli* (UTI89) and the absence of Hfq causes reduction in microcolony formation in the bladder and kidneys (26).

Although Hfq is a central player in sRNA-mediated gene regulation, how it facilitates these RNA interactions is yet to be discovered. A number of findings suggest that Hfq binds sRNA and target mRNA simultaneously using two independent binding faces (Figure 2) (21,28). The proximal face interacts with sRNA by binding to single-stranded A/U rich regions while both faces contact the mRNA. The distal face preferentially binds to ARN tracts (where A is an adenine, R is a purine and N is any nucleotide) on mRNA (21,29). It has been found that Hfq increases sRNA interaction with their target mRNAs by bringing both RNAs together (29,30). Table 1 shows some of the examples of sRNA-mRNA interactions which are formed under stress conditions in an Hfq dependent manner (13,15,16). sRNAs that are relevant for the present study are marked with asterisks. The regulatory roles of these sRNAs are discussed below.

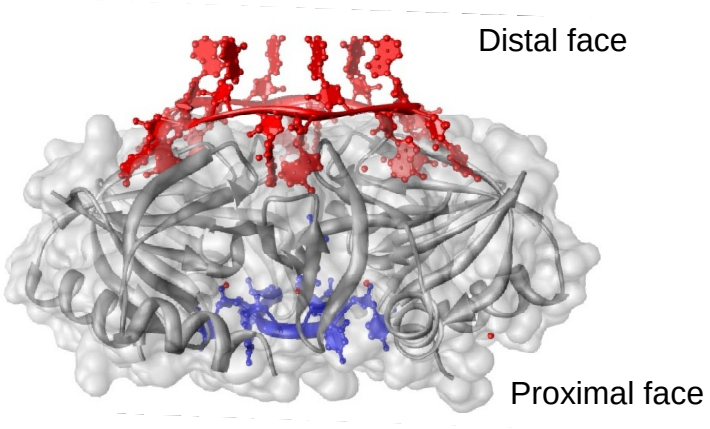

Figure 2: Hfq-RNA interactions. Hfq proximal face interacts with sRNA while distal face interacts with mRNA. Crystal structure shows distal face bound to A_6 and proximal face bound to AU_5G (21).

Table 1: Examples of sRNA-mRNA interactions formed under stress conditions.

Stress condition	sRNA	Target mRNA	Regulatory outcome
Cold shock	RprA	*rpoS*	Translational activation
	DsrA*	*rpoS*	Translational activation
		hnS	Translational repression
Oxidative stress	OxyS*	*fhlA*	Translational repression
		rpoS	Translational repression
Nutrient levels	MicC	*ompC*	Translational repression
	GcvB	*oppA/dppA*	Translational repression
Heat shock/toxins	MicF	*ompF*	Translational repression
Low glucose	Spot42	*galETKM*	Translational repression
Sugar stress	SgrS*	*ptsG*	mRNA degradation
Low iron	RyhB	*sodB*	mRNA degradation
		sdhCDAB	mRNA degradation

OxyS-Hfq regulates gene expression under oxidative stress

Reactive oxygen species such as hydrogen peroxide, superoxide and hydroxyl ions are produced continuously inside the cells as by-products of cellular reactions. These reactive oxygen species can initiate a series of radical reactions, which can damage cellular macromolecules. Lipids, proteins and DNA are major targets of reactive oxygen radicals. The broad spectrum of damage includes amino acid adduct formation by oxidation of metal binding sites in enzymes, biomolecule fragmentation and DNA mutations which can be fatal for the cells (31). Therefore, cells have evolved a number of defense mechanisms including repression of certain genes, to reduce the production of reactive oxygen species.

The transcriptional activator, OxyR is activated in cells stressed by peroxides. OxyR activates the expression of defensive proteins and regulatory

RNA OxyS to protect the cells against oxidative damage (32). It has been shown that 109 nt long OxyS untranslated RNA represses the translation of *rpoS* (encodes sigma factor σS) and *fhlA* (encodes a transcriptional activator of formate metabolism) (18,30). The base-paring of OxyS to its target *fhlA* mRNA, prevents ribosome binding to the mRNA thus it inhibits the translation of the protein allowing the organism to recover from the oxidative stress (11,18,30).

DsrA is a multiple RNA regulator under cold shock.

DsrA is an 85 nt long trans-acting small RNA, which is synthesized under cold shock and is involved in the translational activation of *rpoS* (Figure 1) and the translational repression of *hns* which encodes for histone-like protein, HNS (30). RpoS is an *E.coli* stationary phase sigma factor that binds to the RNA polymerase to initiate the transcription of many stress responsive genes which are stimulated by carbon starvation, low temperatures, pH changes and high osmolarity (33). Under normal growth conditions the *rpoS* 5'UTR forms a secondary hairpin structure that occludes the ribosome binding site (RBS); thus, it inhibits the translation of RpoS. During cold shock, DsrA remodels the *rpoS* inhibitory structure by base-pairing to the *rpoS* leader sequence. This releases the RBS and activates translation of the protein (34). It has been found that Hfq facilitates these regulatory processes by bringing the two RNAs together and stabilizing the final RNA-RNA complex (11,21,35). In contrast, DsrA represses *hns* mRNA by making the DsrA-*hns* duplex that overlaps the start codon of the

hns mRNA and prevents the translation of HNS (30,36). Thus, DsrA regulates the expression of at least two mRNAs, highlighting the complexity of the sRNA mediated regulatory network (11,28,30).

SgrS-Hfq paring with *ptsG* mRNA leads to degradation of both RNAs

In addition to translational activation and translational repression, target degradation is another common outcome of sRNA-mRNA interactions. SgrS is a small RNA that is transcribed during sugar phosphate stress, which is induced by the accumulation of glucose-6-phosphate (G-6-P) (11,16). Glucose or α-methyl-glucose transports into the cells via the PtsG glucose transporter and are phoshorylated into glucose phosphate or α-methyl-glucose phosphate by the phospho transferase system (PTS). When the glycolytic pathway is disrupted or non-metabolizable α-methyl-glucose phosphate is present, cells undergo sugar-phosphate stress which gives the signal to the SgrR transcriptional activator to synthesize SgrS small RNA (Figure 3). SgrS base pairing to *ptsG* mRNA leads to translational repression followed by the degradation of *ptsG* mRNA by RNase E. Hence, it inhibits the synthesis of the glucose transporter, PtsG, and allows cells to maintain sugar phosphate tolerance (16,37,38). This process is known to be facilitated by Hfq and it is believed that association of SgrS with RNase E takes place through Hfq (39).

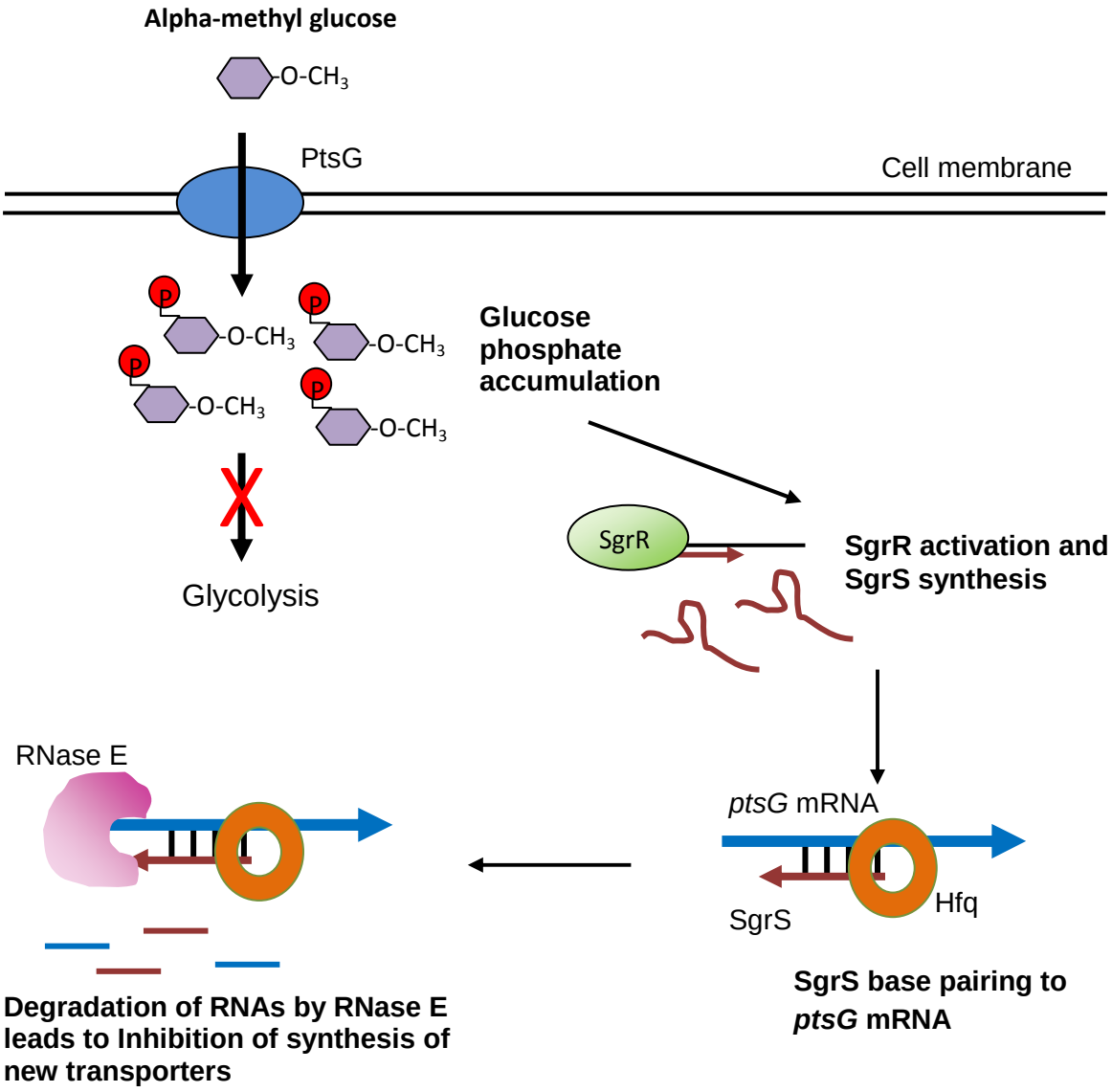

Figure 3: Sugar phosphate tolerance in bacteria. Glucose or α-methyl-glucose transports into the cells via the PtsG glucose transporter. When the glycolytic pathway is disrupted or non-metabolizable α-methyl-glucose is present, cells undergo sugar-phosphate stress due to the accumulation of glucose phosphate or α-methyl-glucose phosphate. This gives the signal to the SgrR transcriptional activator to synthesize SgrS small RNA. SgrS base pairing to *ptsG* mRNA leads to the degradation of *ptsG* mRNA by RNase E. Hence, it inhibits the synthesis of the glucose transporter, PtsG, and allows cells to maintain sugar phosphate tolerance (16,37,38).

Hfq interacts with other proteins to mediate its regulatory roles

Several studies have shown that Hfq makes Hfq-RNP complexes to mediate its regulatory roles (11,40,41). It has been reported that Hfq interacts with the RNA degradation machinery and may direct the sRNA-mRNA complex for degradation (11,41). In support of this hypothesis, co-immunoprecipitation experiments have shown the existence of an Hfq-RNase E complex (41). Hfq is also known to interact with PAPI and PNPase to form a complex that is distinct from the degradosome which is involved in polyadenylation of mRNAs (42). A recent paper showed that Hfq interacts with the *Salmonella typhimurium* virulence factor PhoP, a component of PhoPQ system which plays a role in *Salmonella* pathogenesis (43,44).

An RNA affinity column approach followed by LC-MS and MALDI-TOF analyses identified many proteins that make direct/indirect contacts with Hfq (Lee and Feig unpublished data). Previous work in our lab used three small RNAs as bait to fish out the proteins that are in complex with Hfq. Most of them were RNA binding proteins which have already been shown to bind Hfq. RhlE is a DEAD-box helicase and was identified as a protein partner in SgrS-Hfq and DsrA-Hfq RNP complexes where SgrS and DsrA were used as bait to hire Hfq and its protein partners (Figure 4). For many years, it has been assumed that Hfq lacking ATPase activity, requires the help of an RNA helicase to remodel the structured RNAs in order to facilitate base-paring between sRNA and mRNA.

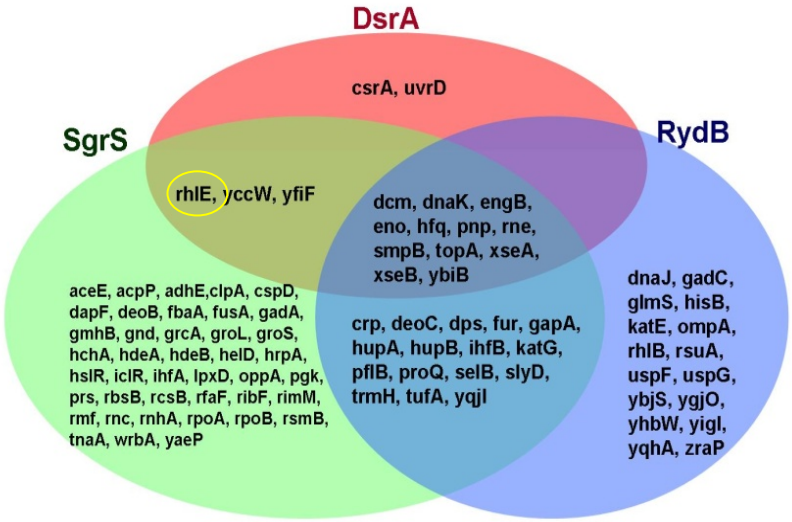

Figure 4: Hfq-RNP complexes. An RNA affinity column approach followed by LC-MS and MALDI-TOF analyses identified many proteins that make direct/indirect contacts with Hfq. RhlE was identified as a protein partner of SgrS-Hfq and DsrA-Hfq RNP complexes. RhlE is highlighted with a circle.

DEAD-box RNA helicases are ATP energy driven motor proteins that are involved in RNA metabolism

DEAD-box helicases are ATP-dependent RNA helicases stimulated by long or short double-stranded RNA molecules (45,46). They are involved in dynamic RNA metabolic processes including ribosome biogenesis, mRNA splicing, and mRNA decay by unwinding RNA secondary structures and rearranging the ribonucleoprotein complexes (47). Based on the sequence conservation of motifs, helicases are divided into six super families; SF1-SF6. SF1 and SF2 family proteins are monomers while SF3-SF6 family proteins form hexameric ring structures (47,48). Despite the classification into six super

families, all the DEAD-box RNA helicases have the same fold to form the conserved DEAD-box core. Thus, they exhibit two main enzymatic activities; RNA unwinding helicase activity and ATPase activity (49).

Although a number of different DEAD-box RNA helicases have been identified in eukaryotes and prokaryotes, full-length crystal structures of most these are not available. MjDEAD from *Methanococcus jannashii* is among the first to be fully characterized (Figure 5). DEAD-box helicases have nine conserved motifs including the Asp-Glu-Ala-Asp motif (D-E-A-D or motif II) (45-47). Four motifs are known to be involved in ATP binding and hydrolysis, while four of the others are involved in RNA binding (Figure 5). Motif three sits in between domains IV and DEAD, and is identified as a linker domain which passes the conformational change induced by ATP hydrolysis to the RNA binding domains (46). Thus, proper coordination among motifs ensures a tight relationship between RNA and ATP binding sites, leading to coupled ATPase and helicase enzymatic activities.

In general, RNA helicases unwind RNA duplexes either by a translocation based mechanism or through local strand separation. In the first mechanism, the helicase binds to the single-stranded 5’ or 3’ overhang of the RNA and translocation occurs towards the duplex in an ATP dependent manner. ATP binding, ATP hydrolysis, and phosphate release occur in each translocation step to move the protein forward (50).

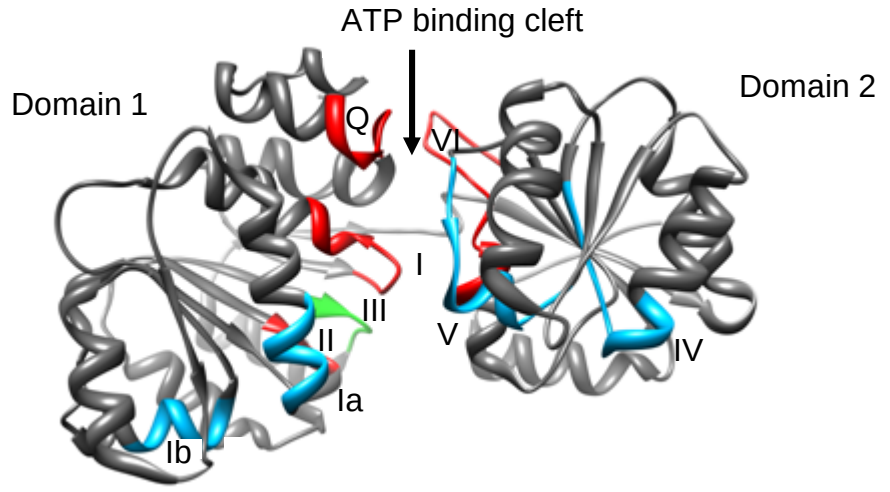

Figure 5: Structure of a DEAD-box helicase (*Methanococcus jannaschii*). The protein contains two domains and nine motifs. ATP binding cleft sits between domain 1 and 2. Motifs Q, I, II (DEAD motif) and VI involve in ATP binding (red) and motifs Ia, Ib and V involve in RNA binding (blue). Motif III (green) acts as a linker which passes the conformational change induced by ATP hydrolysis (47). This image was reconstructed with UCSF chimera using PDB ID 1HV8.

Most DEAD-box RNA helicases follow the second mechanism. They load directly on the double stranded regions with the aid of neighboring single stranded regions. The loading can take place at 3' or 5' end of the duplex or internally by a yet undefined mechanism which is thought to be assisted by ATP binding. Upon ATP binding the enzyme assumes a high affinity RNA binding conformation which allows rapid dissociation of the RNA duplex. ATP hydrolysis weakens RNA binding and leads to dissociation of the two unwound RNA strands and the enzyme (50,51).

E.coli DEAD-box helicase DbpA is an example of such helicase that unwinds duplex rRNAs by a process that requires ATP association and

hydrolysis. A recently published paper showed that ADP-Pi bound DpbA binds to phosphoryl transfer center-RNA and unwinds short rRNA duplexes. The dissociation of the duplex occurs rapidly and is followed by a slow, rate determining Pi release step and the dissociation of the enzyme (51). Figure 6 shows the schematic diagram for *E.coli* DEAD-box helicase, DbpA action (51).

RhlE is an *E.coli* DEAD-box RNA helicase with yet undefined role

E.coli expresses 5 DEAD box helicases: DbpA, SrmB, RhlB, RhlE and CsdA. DpbA and SrmB were reported to be involved in ribosome biogenesis (45,46). Being the regular helicase component of the degradosome, RhlB participates in resolving structured RNAs and facilitating their degradation (45-47,52). It was reported that, under certain growth conditions degradosome components get rearranged. For example, CsdA can replace the function of RhlB at low temperatures (53,54). RhlE is the least characterized among the five and many questions on RhlE await answers.

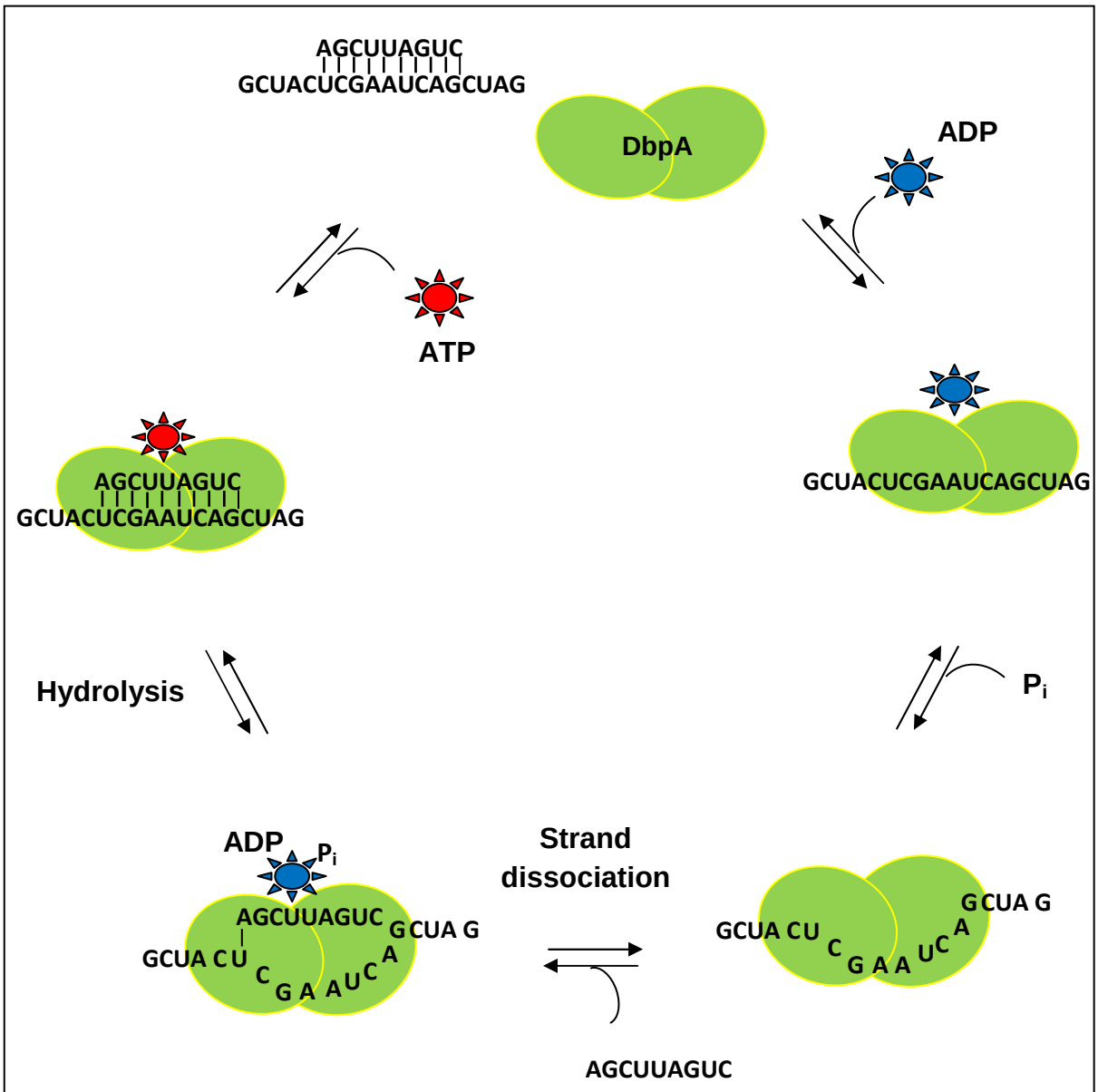

Figure 6: Mechanism of DbpA helicase action. DbpA unwinds duplex rRNAs by a process that requires ATP association and hydrolysis. Upon ATP binding the enzyme assumes a high affinity RNA binding conformation which allows rapid dissociation of the RNA duplex. ATP hydrolysis weakens the RNA binding and leads to the dissociation of the two unwound RNA strands and the enzyme (Reproduced with permission from M. De La Cruz., PNAS *107*(9), 2010).

RhlE may play a role in sRNA-mediated gene regulation under stress conditions

RhlE is characterized as an ATP-dependent RNA helicase. Although its exact function(s) or substrate(s) *in vivo* is not known, it was reported that, like CsdA, RhlE also interacts with RNase E without displacing RhlB (55). Ribosome analysis and primer extension assays have shown that RhlE can suppress the growth defects that are associated with ribosome biogenesis in SrmB mutants at cold temperatures (52). In addition to their role in resolving structured RNA molecules, recent work has suggested that the DEAD-box RNA helicases can act on RNP complexes to displace proteins and rearrange the RNP complexes (47,56).

All the DEAD-box RNA helicases in *E.coli* show slow enzymatic activities *in vitro (45)*. To explain this fact, it has been proposed that, these enzymes act on highly specific substrates *in vivo* and work together with other proteins to achieve their substrate specificity and high processivity.

RhlE has distinct features relative to the other four DEAD box helicases. RhlE is reported to be the most processive enzyme *in vitro (45,56)*. Furthermore, like other RNA helicases found in *E.coli,* RhlE does not require RNA substrates with 5' or 3' overhangs for its helicase activity (45). RhlE is able to unwind short/ long or blunt end duplexes.

Considering all these facts, RhlE can be considered as a potential candidate for the helicase component of the 'stress-induced degradosome'. Our hypothesis in this study was that RhlE and Hfq have a synergistic effect on

sRNA-mediated gene regulation under stress conditions. Thus, it is worthwhile to address the following questions.

1. Does RhlE play a role in sRNA-mediated gene regulation?
2. Does the deletion of *rhlE* make any change in the growth phenotype of the *hfq* mutants?
3. Does RhlE interact with Hfq to mediate these regulatory outcomes?
4. How does Hfq facilitate base pairing of structured RNAs?
5. What is the mechanism of RhlE action?

Hfq may recruit a protein partner, which has the ability to resolve RNA secondary structures (RhlE?). In order to answer the above questions, a series of *in vivo* and *in vitro* experiments were performed which are discussed below.

Project Outline

Our goal is to understand the effect of RhlE and Hfq on gene regulation in bacteria during stress responses and to characterize the role of Hfq as a regulator of sRNA-mRNA interactions. We hypothesized that Hfq and RhlE have a synergistic effect on sRNA-mediated gene regulation. To address this problem, a series of *in vivo* and *in vitro* experiments were carried out. To study the effect of RhlE and Hfq on sRNA mediated gene regulation, *ΔrhlE* and *ΔrhlE/Δhfq* knockout strains were constructed and their growth patterns were examined under different stress conditions. In a previous study, RhlE was identified as a protein partner of the Hfq-SgrS and Hfq-DsrA protein complexes. Co-

immunoprecipitation was used to find the existence of possible Hfq-RhlE complex. *In vitro* ATPase assays were used to demonstrate the ability of RhlE to act on different sRNAs and potential mRNA substrates. The ability of Hfq to stimulate the ATPase activity of RhlE, with or without relevant RNAs present, was tested.

In the present study, the growth curve analysis of wt, *ΔrhlE, Δhfq* and *ΔrhlE/Δhfq* revealed that RhlE has a role in Hfq-dependent sRNA-mediated gene regulation under sugar stress and oxidative stress. It was also found that OxyS sRNA, which is transcribed under oxidative stress, and its target *fhlA* mRNA stimulate the ATPase activity of RhlE. Furthermore, DsrA was unable to stimulate RhlE, suggesting that RhlE may have some degree of specificity for RNAs. Although Hfq was shown to stimulate the RhlE ATPase activity in the presence of *fhlA*, the present study did not identify any physical interaction between the two proteins.

CHAPTER TWO

MATERIALS AND METHODS

Materials

All chemicals and reagents used were reagent grade or better. LB broth and LB agar was purchased from EMD Chemicals Inc. Hydrogen peroxide, NaCl, $MgCl_2$, KCl, HEPES, PBS, Tris-HCl and dNTP mix were bought from Fisher Scientific. Glucose, NADH, phosphorenolpyruvate, pyruvate kinase, lactate dehydrogenase, ATP, agarose, IPTG, arabinose, triton-X and imidazole were purchased from Sigma. Alpha-methyl glucose was bought from Fluka. Transcription and PCR buffers and enzymes were purchased from NEB Biolabs. Hi-tap Ni^{2+} columns were bought from GE Healthcare. Plasmid miniprep kit and PCR cleanup kit were purchased from Qiagen. EDTA-free protease inhibitor tablet is from Roche Diagnostic and Dyna-beads are from Invirogen. Anti-v5 and anti-his probes were purchased from Sigma. All the primers were purchased from IDT.

Media and growth conditions

Cells were grown under aerobic conditions at 37^{o}C (except for conditions where cells were induced by cold shock (30^{o}C) or heat shock (42^{o}C)) in LB broth. To induce stress conditions, media were supplemented with 0.25%, 0.5%, 0.75% or 1% α-methyl glucose for sugar stress, 60μM H_2O_2 for oxidative stress or 0.5M NaCl for osmotic pressure when required. Antibiotics were added at 30 μg/mL

kanamycin, 100 µg/mL ampicillin, 34 µg/mL chloramphenicol and/or 100 µg/mL streptomycin.

Strains and plasmids

All deletion mutants were derived from *E.coli* Top10 cells. λ Red–mediated recombination was used to generate single and double knockout strains containing deletions within *hfq* and *rhlE* genes. *hfq* or *rhlE* were replaced with cassettes that have kanamycin and chloramphenicol resistant genes respectively. Amplified FRT-cam/kan cassette using PCR primers; ISRHK01 and ISRHK02 (Table 2) with homologous flanking arms containing 50bp of upstream and downstream regions of *rhlE/hfq* gene were transformed into Top10 electrocompetent cells. The insertion of the antibiotic cassettes into correct position was confirmed by PCR. All the knockout strains constructed for this study are listed in table 3.

The *rhlE* gene (1365bp) was amplified using GM 30 genomic DNA as the template and primers ISRH01 and ISRH02 (Table 2). The PCR amplified gene fragment was inserted into pET28a via *NdeI* and *HindIII* restriction sites in frame with N-terminal His-tag (pMIS20201) (Table 4). Clones were selected by kanamycin resistance. Correct insertion of the gene into pET28a was confirmed by restriction digestions and sequencing. To express RhlE, pMIS20201 was transformed into BL-21(DE3).

For co-immunoprecipitation experiments, *V5* tagged *rhlE* containing plasmid (pMISV520201) was created (Table 4). The *rhlE* gene was PCR amplified using a reverse primer IRSHV02 (Table 2) containing the coding sequence for V5 epitope, immediately after the last sense codon of *rhlE* followed by the stop codon. The PCR product was ligated into pBAD24 and transformed into Δ*rhlE*. Resultant strain was named as IRV 002 (Table 3).

Table 2: Primers used in this study.

Primer name	**Target gene / Purpose**	**Location (respect to RhlE start codon)**
ISRH01	RhlE / PCR amplification	+1 ⟶ +26
5’ GGAACCCATATGTCTTTCGATTCTTTGGGTTTAAG 3’		
ISRH02	RhlE / PCR amplification	+1362⟶+1342
5’ TAGCTCAAGCTTACTGCGCAGCGGCAGGTTTAC 3’		
ISRH03	RhlE sequencing	+625 ⟶ +648
5’ ACCTTCTCTGACGATATTAAAGC 3’		
ISRHK01	RhlE knockout	-50 ⟶ 0
5’ TATCTCCCTGAAAACTACACCGGTAACGGTCGGGGC GGTTCGGAGTAGTTAATTAACCCTCACTAAAGGGCG 3’		
ISRHK02	RhlE knockout	+1365⟶+1415
5’TTTTGCGTTTGTTCATCAGCCTGATGCCGGGCATAGC CCGGCATAAAAGATAATACGACTCACTATAGGGCTC 3’		
ISRHV02	RhlE-V5	+1362⟶+1341
5’AAGAAGAAGCTTTTAGGTGCTATCAGGCCCAGCGGGTT CGGAATCGGTTTGCCCTGCGCAGCGGGCAGGTTTACG 3’		
Kan-Int	Kanamycin/PCR confirmation of Δ*hfq*	Internal
5’ TGATATTCGGCAAGCAGGCATC 3’		
Cam-Int	Chloroamphenicol / PCR confirmation of Δ*rhlE*	Internal
5’ TCACCGTCTTTCATTGCCATACG 3’		

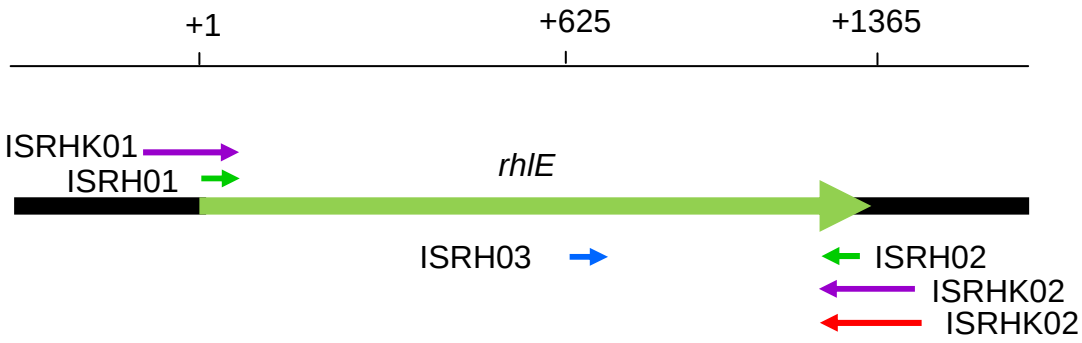

Figure 7: Positions of the PCR primers used in this study. Arrows indicate the direction and the relative size of the primer. *rhlE* gene was amplified using ISRH01 and ISRH02 (green) primers and inserted into pET28a vector. ISRHV01 and ISRHV02 (purple) carry homologous flanking arms containing 50bp of upstream and downstream regions of *rhlE* gene and were used to construct knockout strains. ISRH03 (blue) was used for sequencing and confirmation of *rhlE* konckouts. ISRHK02 (red) carries sequence for V5 epitope.

Table 3: Strains used in the study.

Name	Parent strain/ Gene(s) deleted	Resistance	Comments
E.coli MG1665	Wild type	-	-
BL21(DE3)	*E.coli* F^- ompT gal dcm lon $hsdS_B$ (r_B^- m_B) λ(DE3 [lacI lacUV5-T7 gene 1 ind1 sam7 nin5])	-	Carries T7 RNA polymerase gene under UVlac promoter and lacI
BL21(DE3)	BL21(DE3)/ pMIS20201	kan^{Δ}	Expresses His-tagged RhlE
E.coli Top10	F- *mcr*A Δ(*mrr-hsd* RMS-*mcr*BC) φ80*lac* ZΔM15 Δ*lac*X74 *rec*A *ara*D139 Δ (*araleu*) 7697 *gal*U *gal*K *rps*L (StrR) *end*A1 *nup*G	Strep*	-
IR001	*E.coli* Top10/ Δ*hfq*	Kan^{Δ}	Shows slow growth phenotype in LB at 37°C
IR002	*E.coli* Top10/ Δ*rhlE*	$Cam^{\#}$	No obvious growth defect compared to wt
IR003	*E.coli* Top10/ Δ*rhlE*/ Δ*hfq*	Kan^{Δ}/$Cam^{\#}$	Shows slow growth phenotype in LB at 37°C as Δ*hfq* does
IRV002	IR002 contains pMISV20201	Kan^{Δ}/$Cam^{\#}$ Amp^{Φ}	No obvious growth defect compared to wt

*streptomycin $^{\Delta}$Kanamycin $^{\#}$ Chloroamphenicol $^{\Phi}$Ampicilin

Table 4: Plasmids constructed for this study.

Name	Parent plasmid	Resistance	Restriction sites	Size (bp)	Comments
pMIS20201	pET28a	Kan	*Nde1/HindIII*	6671	N-terminal His tag
pMISV20201	pBAD24	Amp	*EcoR1/HindIII*	5949	C-terminal V5 tag

Effect of rhlE and hfq on growth under stress conditions

Δ*hfq,* Δ*rhlE* and Δ*rhlE*/Δ*hfq* strains were subcultured from an overnight culture and cells were grown to mid log phase (OD_{600}~0.4-0.6). Cells were diluted into fresh pre-incubated LB with appropriate antibiotic(s) (3 from each strain) to have the initial OD_{600} ~ 0.02 (time = 0). Cells were stressed by the supplementation of 0.25%,0.5%, 0.75% or 1% α-methyl glucose for sugar stress, 60 µM H_2O_2 for oxidative stress or 0.5 M NaCl for osmotic pressure to the medium. Growth was followed by measuring OD_{600} every hour. To induce cold shock or heat shock conditions, cells were grown at 30^{o}C or 42^{o}C respectively. The log of OD_{600} vs time (h) was plotted for the log phase of the growth curve and the growth rate (k) was determined by the slope. Doubling time for each strain was calculated by µ= log (2/k). Mean doubling time of two or more independent trials were taken into account for the analysis. Data were analyzed statistically using student's t-test to determine if there is a significant difference between the doubling times.

Expression and purification of RhlE-His

BL-21(DE3) cells containing pMIS20201 were grown to OD_{600}~0.4 and induced with 1 mM IPTG for 3 hours at 37^{o}C. Purification procedure was modeled after that of Bizerbard *et al.* in 2004. Cells were harvested, resuspended in RhlE binding buffer (300 mM KCl, 10 mM HEPES and 10 mM Immidazole) and half of EDTA-free protease inhibitor cocktail tablet (Roche) was added per 1 L of culture. Lysate was prepared by sonication of cells on ice followed by centrifugation at 15,000 g for 30 min at 4℃. The sup ernatant was filtered through 0.2 µm filter (PAL life sciences) and the filtrate was loaded on a Hi-Tap Chelating Ni-column charged with 100 mM Ni^{2+}. Extensive washings with RhlE wash buffer I (300 mM KCl, 10 mM HEPES and 50 mM Imidazole) was carried out to remove non-specific binding followed by additional washing steps with RhlE wash buffer II (300 mM KCl, 10 mM HEPES and 1 M urea) and RhlE wash buffer III (300 mM KCl, 10 mM HEPES and 1 M KCl). His-tagged protein was eluted using RhlE elution buffer (300 mM KCl, 10 mM HEPES and 300 mM Imidazole). Protein was eluted with minute amounts of contaminant proteins. To remove the contaminant proteins, FPLC sizing column was used. Pre-equilibration of the column was done with RhlE binding buffer without Imidazole. FPLC elution fractions were passed through a second Ni^{2+} column to concentrate the protein, dialyzed against RhlE storage buffer (75 mM KCl, 10 mM Hepes pH 7.5, 0.1 mM EDTA, 1 mM DTT) and the concentration was determined by absorbance at 280 nm.

RNase Test

To check for the RNase contaminations in the purified protein, RhlE (0.5 µM) was mixed with 0.1 µM DsrA, incubated for 4 hours at 37^{o}C, and visualized on a denaturing PAGE (10%) gel. No significant degradation of RNA was observed.

Determination of activity of RhlE and *in vitro* ATPase assays

To determine the activity of the protein, ATPase assay was employed. ATPase activity was measured using lactate dehydrogenase/pyruvate kinase coupled enzyme assay. NADH depletion was monitored by decrease in absorbance at 340 nm. The concentrations used in the assay were as follows (45).

Table 5: ATP assay components and their concentrations.

Component	Concentration (stock)	Concentration
Pyruvate kinase	265 U/mL	10 U/mL
LDH	387 U/mL	20 U/mL
ATP	100 mM	1.25 mM
$MgCl_2$	25 mM	0.5 mM
PEP	5 mM	200 µM
NADH	10 mM	100 µM
RhlE	7.5 µM	0.3 – 0.5 µM
Assay Buffer	75 mM KCl, 10 mM	75 mM KCl, 10 mM

Spectrometric measurements were made by UV-Vis 8453 spectrophotometer (Agilent). Reaction time was 5 min. Poly A, is known to be a strong stimulator of RhlE (45). A_{18} was used to check the activity of purified

protein. DsrA, OxyS and *fhlA* were used as RNA components in *in vitro* ATPase assays and the effect of Hfq on RhlE was tested by adding Hfq. This experiment was done at two different RNA concentrations (40 nM-600 nM) in the precense of 0 nM and 1000 nM Hfq. A reaction which excludes RhlE was considered as background. Spectroscopic data were analyzed using Kaleidagraph software.

Co-immunoprecipitation

Δ*rhlE* and IRV 002 were grown to mid log phase and IRV 002 was induced by 0.01% arabinose. Total protein extracts were made by sonication of cells in lysis buffer, followed by centrifugation at 15,000 rpm at 4^{o}C for 30 min. Anti-hfq antibody (1/10000) was pre-incubated with Protein A dynabeads for 30 min at 25^{o}C and the cell lysates were mixed with the anti-hfq bound Protein A beads. Mixtures were rotated for overnight at 4^{o}C. Following incubation, beads were extensively washed with 1X PBS buffer with 0.02% Tween 20, transferred to a new tube, mixed with SDS-gel loading buffer and boiled for 45 min. Eluted proteins were run on a SDS-PAGE gel, transferred to a nitrocellulose membrane at 90V, 30mA for overnight and were probed with anti-V5 anti body.

CHAPTER THREE

RESULTS

rhlE deletion does not affect the growth of wild type *E.coli*

To test the effect of RhlE on *E.coli* growth, wt, Δ*rhlE*, Δ*hfq,* and Δ*hfq*/Δ*rhlE* cells were grown in LB broth at 37^{o}C. The growth of Δ*rhlE* was compared to that of the wild type and the growth of Δ*hfq*/Δ*rhlE* was compared to that of the Δ*hfq.* Hfq mutant strains show multiple growth defects including slow growth rates even in rich media (24). As expected, *hfq* knockouts showed decreased growth rates at all temperatures and stress conditions used (Figure 8). Consistent with the literature Δ*rhlE* showed no significant growth defect at 37^{o}C (56). Furthermore, *rhlE* deletion did not affect the slow growth rate of Δ*hfq*.

Δ*hfq*/Δ*rhlE* did not exhibit a significant growth difference from Δ*hfq* under cold shock, heat shock or osmotic pressure

Hfq mediates sRNA–mRNA interactions in response to regulatory signals which are stimulated by high or low temperatures, osmolarity, pH changes, starvation or non-metabolizable nutrients and chemicals that produce reactive oxygen species and helps bacteria to adapt to extreme environmental conditions (11,57). In order to determine the effect of *rhlE* in stress-dependent regulatory pathways, the growth of Δ*rhlE* was compared to that of the wt and the growth of

Δ*hfq*/Δ*rhlE* was compared to that of the *Δhfq* under different stress conditions (cold shock, heat shock, osmolarity, sugar stress and oxidative stress).

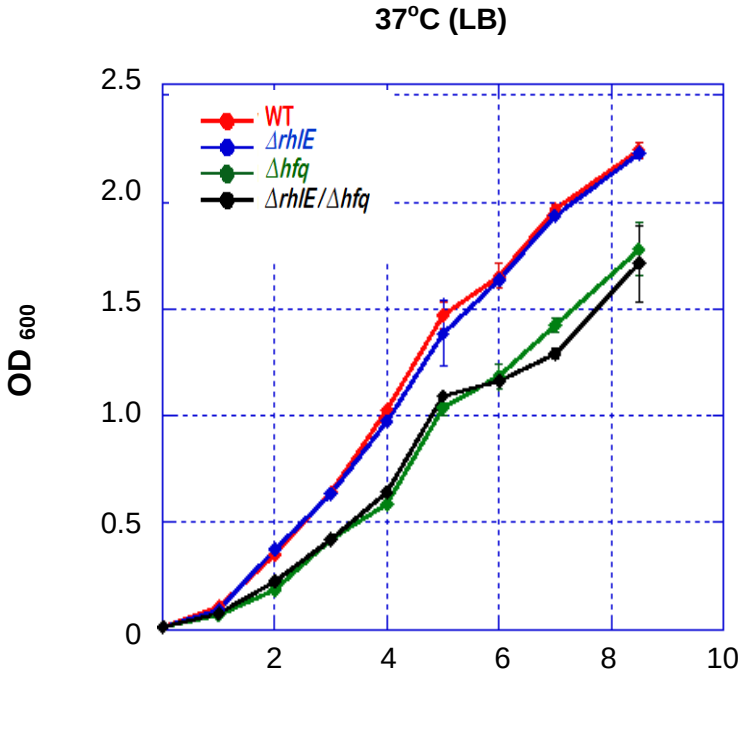

Figure 8: Effect of RhlE and Hfq on growth of *E.coli* at 37°C. Wt, Δ*rhlE*, Δ*hfq,* and Δ*hfq*/Δ*rhlE* were grown in LB broth at 37°C. Cells grown to mid log phase were diluted into fresh pre-incubated LB to have the initial OD_{600}~ 0.02 (time = 0). Growth was followed by measuring OD_{600} every hour. Each data point represents the average of three independent OD_{600} values in which triplicate samples were measured. Error bars represent the standard deviation of three OD values.

Previous work in our lab identified RhlE as a component of DsrA-Hfq and SgrS-Hfq RNP complexes. Under the cold shock condition, which is triggered by low temperatures, DsrA sRNA regulates the expression of multiple mRNAs in an Hfq dependent manner (58). Therefore it was hypothesized that RhlE may play a role in DsrA dependent cold shock responses. To test this hypothesis, wt, Δ*rhlE,* Δ*hfq* and Δ*hfq/*Δ*rhlE* cells were grown at 30^{o}C. However, a significant effect of *rhlE* deletion on growth rates of wt and Δ*hfq* was not observed (Figure 9).

To compare the growth of wt, Δ*rhlE,* Δ*hfq* and Δ*hfq/*Δ*rhlE* strains under osmotic pressure, 0.5 M NaCl was added to the medium and cultures were grown at 37^{o}C. The data did not show a statistically significant difference ($p>0.05$) in doubling times of Δ*rhlE* compared to wt and Δ*hfq/*Δ*rhlE* compared to Δ*hfq* (Figure 10). Further the deletion of *rhlE* did not significantly affect the growth rate of Δ*hfq/*Δ*rhlE* than *hfq* mutants under the heat shock (42^{o}C) (Data not shown).

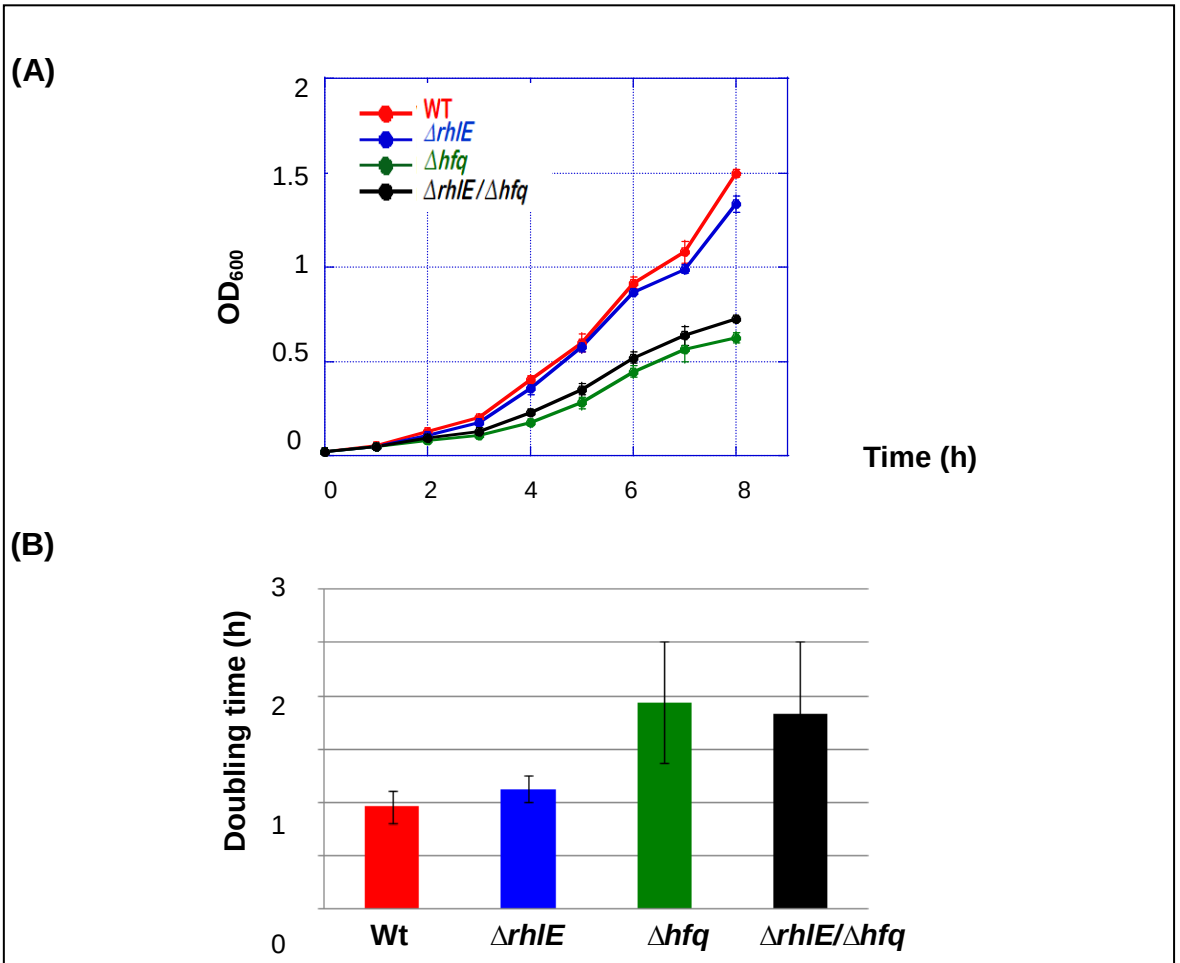

Figure 9: Effects of RhlE and Hfq on *E.coli* growth at 30°C. *rhlE* deletion does not show a significant effect on the growth of wt and Δ*hfq.* (A) Wt, Δ*hfq,* Δ*rhlE* and Δ*rhlE*/Δ*hfq* strains grown to mid log phase (OD_{600}~0.4-0.6) were diluted into fresh pre-incubated LB to have the initial OD_{600} ~ 0.02 (time = 0). To induce cold shock, cells were grown at 30°C. The growth was followed by measuring OD_{600} every hour. Each data point represents the average of three independent OD_{600} values in which triplicate samples were measured. (B) Each column represents the mean doubling time of two independent experiments. Error bars indicate the standard errors of doubling times

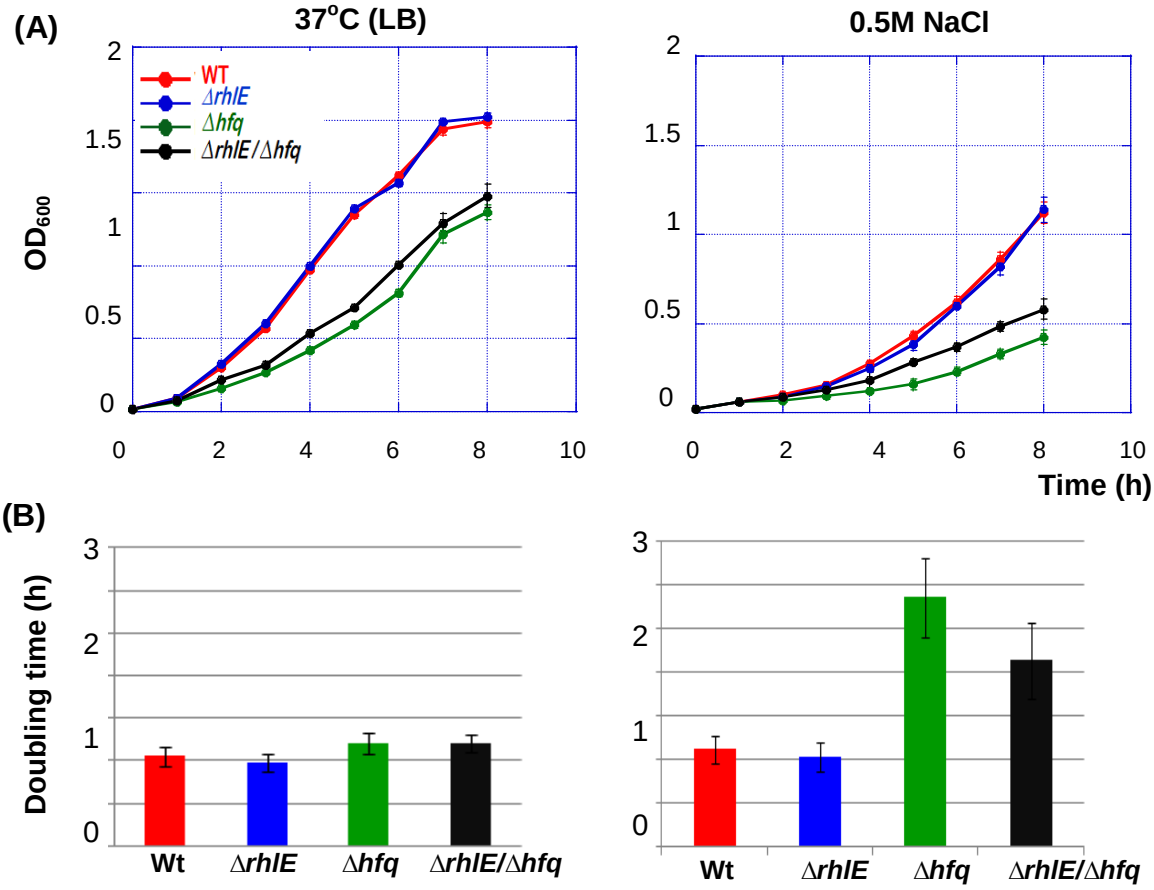

Figure 10: Effects of RhlE and Hfq on *E.coli* growth under osmotic pressure. Wt, *Δhfq, ΔrhlE* and *ΔrhlE/Δhfq* strains grown to mid log phase (OD_{600}~0.4-0.6) were diluted into fresh pre-incubated LB to have the initial OD_{600}~ 0.02 (time = 0). To induce osmotic stress, media were supplemented with 0.5M NaCl. The growth was followed by measuring OD_{600} every hour. (A) Each data point represents the average of three independent OD_{600} values in which triplicate samples were measured. (B) Each column represents the mean doubling time of three independent experiments. Error bars indicate the standard errors of doubling times.

Δ*hfq*/Δ*rhlE* is able to cope with sugar phosphate stress

RhlE was identified as a component of the SgrS-Hfq RNP complex. SgrS base pairing to *ptsG* mRNA leads to translational repression followed by the degradation of RNAs by RNase E which in turn inhibits the synthesis of the glucose transporter, PtsG- IICBGlc and allows the organism to recover from sugar stress (16,37,38). It was proposed that Hfq makes protein-protein interactions with the RNA degradation machinery and may direct the sRNA-mRNA complex for degradation (11,41). Further, it was reported that RhlE interacts with RNase E (55). Therefore it is reasonable to hypothesize that RhlE might have a specific role in the Hfq directed degradation of SgrS-*ptsG* RNA complex. To test if *rhlE* is involved in this regulation, the growth phenotypes of the single and double knockouts in the presence of non-metabolizable α-methyl-glucose were compared. It is known that α-methyl-glucose-6-phosphate is highly toxic to the cells and cells with reduced tolerance to nonmetabolizable sugars show growth inhibition and cell lysis. Therefore, for initial experiments, different concentrations (0.25%,0.5%,0.75% and 1%) of α-methyl-glucose were used. Post induction, this study was performed over 8 hours with OD_{600} measurements collected hourly.

In this experiment, a strong inhibition of the growth in all strains was observed after 4 hours of induction. Cells grown in LB without α-methyl-glucose and in LB supplemented with normal glucose were used as controls. Interestingly, Δ*rhlE*/Δ*hfq* cells showed recovery of the growth after 6 hours while

Δ*hfq* was unable to recover from the stress throughout the experiment time course. (Except at 1% sugar concentration. All four strains showed slow growth at 1% α-methyl-glucose. We suspect that 1% concentration caused cell lysis) (Data not shown).

α-methyl-glucose (0.5%) was selected for further studies in which the experiment was carried out for 15 hours after the induction. OD_{600} was measured every two hour. Three growth trials of wt, Δ*rhlE,* Δ*hfq* and Δ*rhlE*/Δ*hfq* were performed in triplicate. A two stage inhibition pattern throughout the experiment (first after 4 hours and second after 8 hours) was observed and was reproducible (Figure 11).

The current understanding of the SgrS-*ptsG* system is insufficient in explaining the observed growth pattern. Because all the cell types, except Δ*hfq*, followed the same growth pattern, this seems to be an independent event from *rhlE* deletion. One possible explanation for this observed growth pattern is the existence of a selection process that outcompetes individuals incapable of adaptation. After 12 hours of induction all four strains started to show recovered growth. It can be speculated that, by this time the cells have evolved mechanisms to metabolize α-methyl glucose, probably by new enzymes which can remove the methyl group at the anomeric carbon leading α-methyl glucose enter into the glycolytic pathway. However, Δ*rhlE*/Δ*hfq* showed an increased growth rate compared to Δ*hfq* which indicates a possible involvement of *rhlE* on sRNA-Hfq mediated gene regulation under glucose-phosphate stress.

A recent finding suggests that SgrS is not simply a non coding RNA, but it encodes for a small protein SgrT (43 amino acids) (59). This finding gives an additional complexity to the system as SgrT is also involved in maintaining the sugar phosphate tolerance by a mechanism distinct from SgrS (59). Further characterization of the system is required in order to understand the underlying regulatory mechanism and the role of RhlE in this pathway.

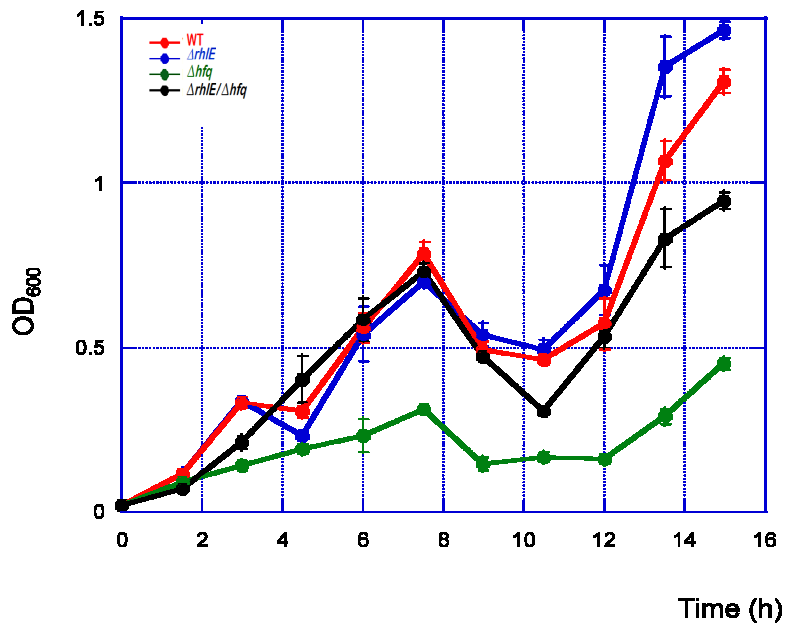

Figure 11: Effects of RhlE and Hfq on *E.coli* growth under sugar-phosphate stress. Wt, *Δhfq, ΔrhlE* and *ΔrhlE/Δhfq* strains grown to mid log phase (OD_{600}~0.4-0.6) were diluted into fresh pre-incubated LB to have the initial OD_{600}~ 0.02 (time = 0). To induce sugar stress, media were supplemented with 0.5% α-methyl-glucose. The growth was followed by measuring OD_{600} every hour. Each data point represents the average of three independent OD_{600} values in which triplicate samples were measured.

rhlE deletion partially restores the slow growth phenotype of Δ_hfq_ under oxidative stress

Defense mechanisms against peroxide-induced oxidative damage partially rely on OxyS-dependent gene regulatory pathways (18). Although Hfq has been characterized as a key player in this regulation, how Hfq acts in this facilitation process is unclear. To test whether RhlE has a role in these regulatory pathways, the growth of Δ*rhlE* and Δ*hfq*/Δ*rhlE* was compared with that of wt and Δ*hfq*. If there is a synergistic effect of RhlE and Hfq proteins in regulating gene expression under oxidative stress, it might be shown in the growth curves as a deviation from the normal growth pattern. Three independent growth trials were performed in triplicate and mean doubling time for each strain was calculated. Interestingly, when oxidative stress was induced by the addition of 60 µM H_2O_2, *rhlE* deletion partially restored the slow-growth phenotype of Δ*hfq* (Figure 12). Statistical analysis of data revealed that the deletion of *rhlE* affects the growth rate of Δ*hfq* significantly ($p<0.05$).

The ability of Δ*rhlE*/Δ*hfq* double knockouts to recover the slow growth phenotype of *Δhfq* suggests that RhlE may have a role in gene regulation under oxidative stress conditions via direct or indirect association with Hfq. To test this, a set of *in vitro* reactions were carried out using the recombinant RhlE protein.

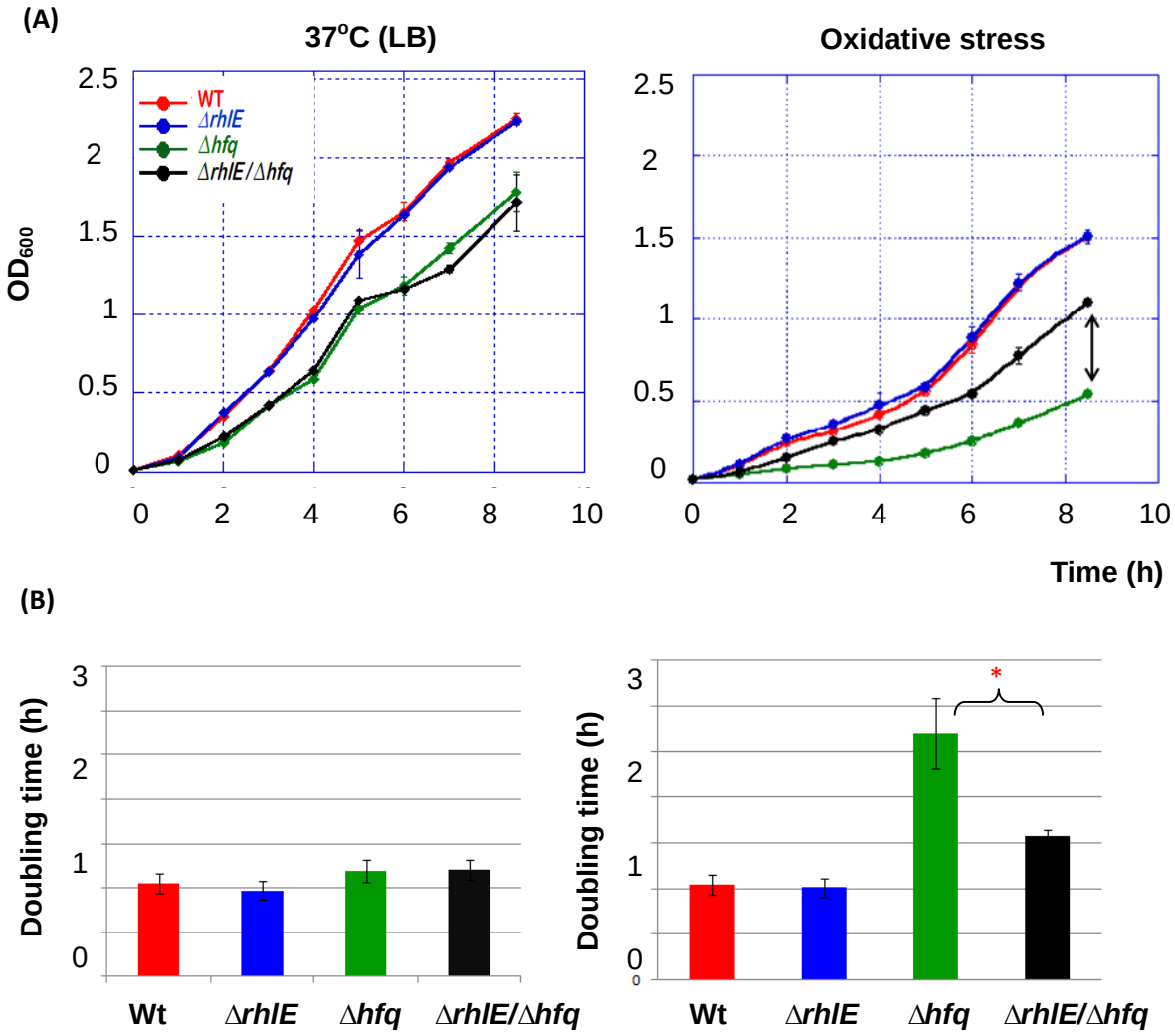

Figure 12: Effects of RhlE and Hfq on *E.coli* growth under oxidative stress. Wt, Δ*hfq,* Δ*rhlE* and Δ*rhlE*/Δ*hfq* strains grown to mid log phase (OD_{600}~0.4-0.6) were diluted into fresh pre-incubated LB to have the initial OD_{600} ~ 0.02 (time = 0). To induce oxidative stress, media were supplemented with 60µM H_2O_2. The growth was followed by measuring OD_{600} every hour. (A) Each data point represents the average of three independent OD_{600} values in which triplicate samples were measured. (B) Each column represents the mean doubling time of three independent experiments. Error bars indicate the standard errors of doubling times. * Indicates $p < 0.05$.

Cloning, overexpression and purification of RhlE

The *rhlE* gene was PCR amplified and cloned into pET28a expression vector in frame with N-terminal His tag, transformed into BL-21(DE3) cells and the protein was overexpressed by the addition of IPTG. His-tagged protein was purified using Hi-Trap Ni^{2+} column, followed by FPLC purification (Figure 13 A). The concentration was determined by the absorbance at 280 nm. To determine if the purified RhlE was free of nuclease contaminations, RhlE was incubated with DsrA for 5 hours and analyzed on denaturing PAGE gel. No degradation of the RNA was observed (Figure 13 B).

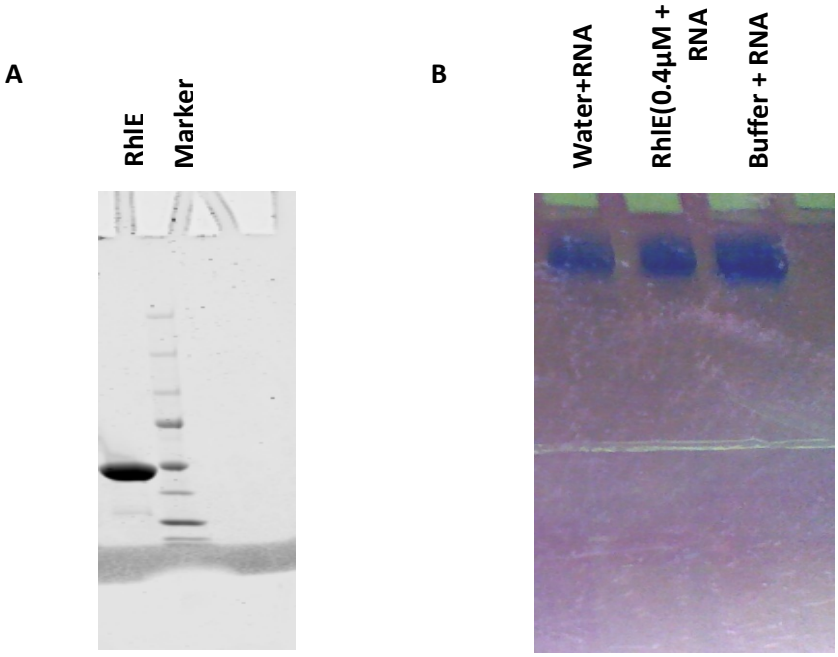

Figure 13: Purification of RhlE. (A) Purified RhlE protein. (B) RNase test. RhlE (0.5µM) was incubated with DsrA, for 4 hours at 37^{o}C, and analyzed on a denaturing PAGE (10%) gel. No significant degradation of RNA was observed.

Isolated protein showed stimulated activity in the presence of A_{18} RNA

To determine whether the protein was active, lactate dehydrogenase/pyruvate kinase coupled enzyme ATPase assay was employed (45). NADH depletion was monitored by the decrease in absorbance at 340 nm in the presence of A_{18} RNA. Poly A has been identified as a good stimulator of RhlE (45). Consistent with the literature, RhlE showed stimulated activity in the presence of $A_{18,}$ yielding a mean rate of 3.5 (± 0.1) x 10^{-3} s^{-1} (Figure 14), and indicated that our purification yielded an active protein.

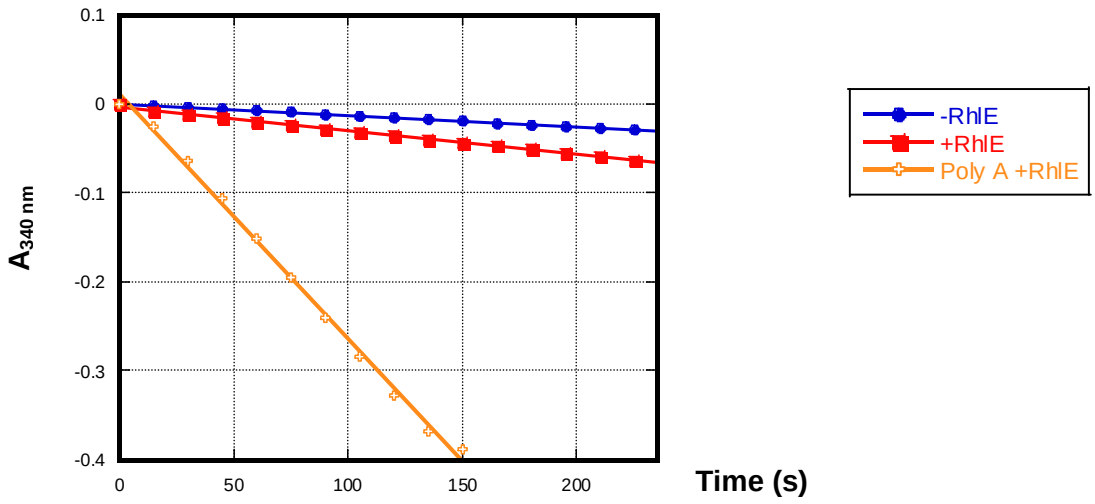

Figure 14: Determination of ATPase activity of RhlE in the presence of A_{18}. ATPase activity of RhlE was measured using lactate dehydrogenase/pyruvate kinase coupled enzyme assay in the presence of A_{18} and absence of RNA substrates. NADH depletion was monitored by decrease in absorbance at 340 nm. The figure represents the best fit of two independent trials. RhlE showed stimulated activity in the presence of A_{18} yielding a mean rate of 3.5 (± 0.1) x 10^{-3} s^{-1}. In the absence of an RNA substrate rate was 1.4 (± 0.1) x 10^{-4} s^{-1}. Blank without RhlE was considered as the background and was subtracted from the measurements.

fhlA and OxyS stimulate RhlE ATPase activity

OxyS base pairing to *fhlA* inhibits the translation of the activator FhlA under oxidative stress (18). The finding that Δ*rhlE*/Δ*hfq* showed partial recovery from oxidative stress compared to the Δ*hfq* knockouts suggests that *fhlA* and OxyS may be possible substrates for RhlE *in vivo*. To test this hypothesis, ATPase activity of RhlE was monitored in the presence of these RNA substrates. Recent work in our lab identified *fhlA220* (extended upstream region) as a better construct than previously characterized *fhlA53* (60) as it forms a more stable ternary complex with OxyS and Hfq (29). Therefore, *fhlA220* and OxyS were used as RNA substrates in the ATPase assay.

Interestingly, *fhlA220* stimulated RhlE ATPase activity with a mean rate of 3.6 (±0.1) X 10^{-3} s^{-1}, a similar rate as what was observed for A_{18} (Figure 15). This was approximately twenty five-fold faster than the rate observed for RhlE in the absence of an RNA substrate (1.4 (± 0.1) x 10^{-4} s^{-1}). Addition of OxyS also stimulated RhlE activity with a mean rate of 1.30 (±0.03) X 10^{-3} s^{-1}, nearly ten-fold faster rate than RhlE alone. Interestingly, addition of DsrA did not stimulate the ATPase activity of RhlE significantly.

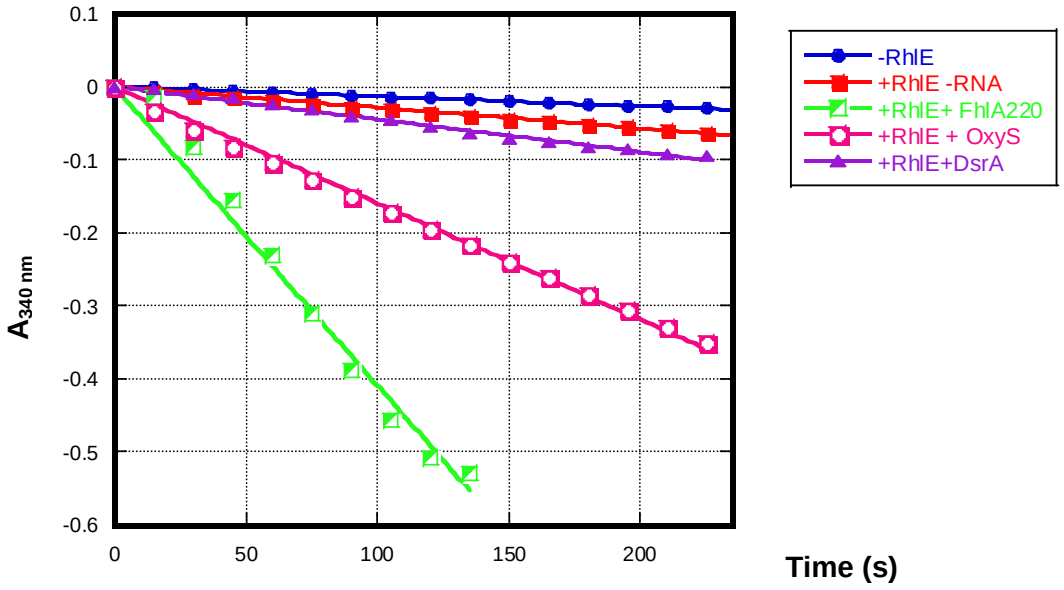

Figure 15: LDH/PK coupled enzyme assay for RhlE in the presence of *fhlA220*, OxyS and DsrA. ATPase activity of RhlE was measured using lactate dehydrogenase/pyruvate kinase coupled enzyme assay in the presence of 600 nM *fhlA220* (green), OxyS (pink), DsrA (purple) and absence of RNA substrates (red). RhlE concentration used was 0.5 µM. NADH depletion was monitored by decrease in absorbance at 340nm. The figure represents the best fit of two independent trials. The mean initial rates were; for *fhlA* = 3.6 (±0.1) X 10^{-3} s^{-1}, OxyS = 1.30 (±0.03) X 10^{-3} s^{-1}, and DsrA = 3.0 (±0.1) X 10^{-4} s^{-1}.

This finding that OxyS but not DsrA stimulates the RhlE ATPase activity indicates that RhlE may preferentially act on selected RNA substrates *in vivo*. Furthermore, these findings suggest a role for RhlE as a potential participant in OxyS-mediated *fhlA* repression under oxidative stress.

Effect of Hfq on RhlE ATPase activity

Hfq facilitates sRNA-mediated regulatory processes under stress conditions (11). In the present study, RhlE was found to be involved in sRNA-mediated regulatory processes under certain stress conditions. To test the effect of Hfq on RhlE's ATPase activity, the assays were done in the presence of 0 and 1 µM Hfq at two different RNA concentrations (40 nM and 600 nM). Previous work in our lab found that K_D for Hfq reaction with *fhlA220* is 15 nM. Therefore, in the presence of excess Hfq concentrations, one can drive *fhlA* to form Hfq-*fhlA* complex. Hence, Hfq-*fhlA* complex acts as the substrate for RhlE contributing predominantly to the overall rate of the reaction. The results shown in the Figure 16 show the influence of Hfq on the rate of conversion of ATP to ADP by RhlE in the presence of *fhlA220*. At 40 nM *fhlA* concentration, the presence of Hfq did not make a significant change in the rate. However, at 600 nM *fhlA* and 1000 nM Hfq, where the concentrations are 10-fold greater than $K_{D,}$ the rate was accelerated, indicating that Hfq can act as a stimulator for the reaction.

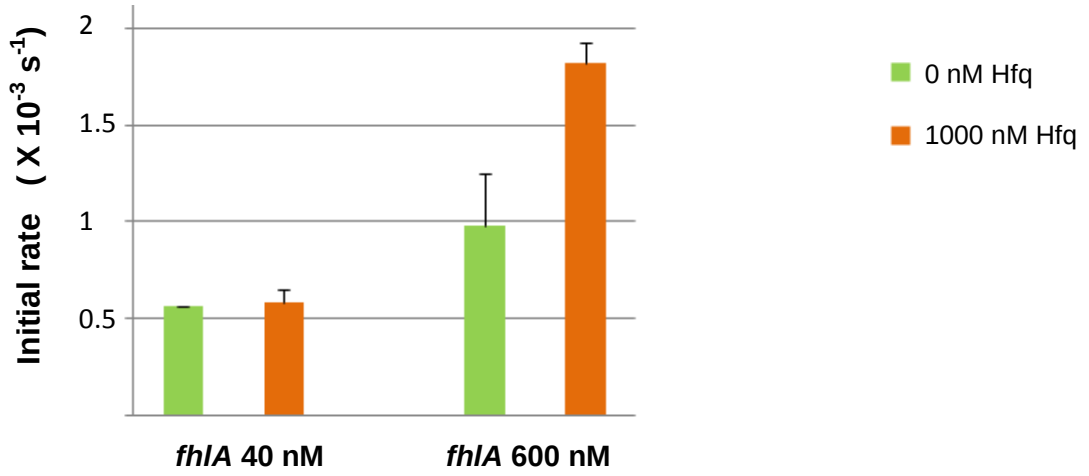

Figure 16: Effect of Hfq on RhlE ATPase activity. ATPase assays were done in the presence of 0 nM and 1000 nM Hfq at two different concentrations of *fhlA* (40 nM and 600 nM). 0.3 µM RhlE was used for the assays. Bars represent the mean rate of two independent experiments.

Hfq does not physically interact with RhlE

The finding that Hfq has an effect on RhlE ATPase activity leads to the hypothesis that these two proteins interact with each other to carry out the regulatory events efficiently. To investigate whether there is a physical interaction between Hfq and RhlE, co-immunoprecipitation experiments were carried out using V5 epitope-tagged RhlE (Figure 17). V5 epitope-tagged *rhlE* was cloned into pBAD24 under arabinose inducible promoter and expressed in Δ*rhlE* (IRV002). IRV002 was inoculated into two fresh cultures and grown to mid log phase. Arabinose (0.01%) was added into both cultures to induce the expression of the protein and 60µM H_2O_2 was added to one culture to induce the oxidative stress. Δ*rhlE* and IRV 002 uninduced were considered as controls. Lysates (L) of

Δ*rhlE*, IRV 002 uninduced, IRV 002 induced with 0.01% arabinose and IRV 002 induced with 0.01% arabinose and 60µM H_2O_2 were incubated with anti-Hfq antibody coated-Dynabeads to pull out Hfq-associated protein complexes. To separate the protein complexes attached to the Dynabeads, a magnetic field was applied and the supernatant (S) was saved for the analysis. Protein complexes attached to the Dynabeads were eluted and run on a SDS-PAGE gel, transferred to a nitrocellulose membrane and were probed with anti-V5 anti body to detect RhlE-V5. If RhlE has a direct interaction with Hfq, a band corresponding to RhlE-V5 should appear on western blot.

RhlE-V5 was readily induced by the addition of 0.01% arabinose (Figure 17, panels (C) and (D) (top) and lighted up in the lysate (L) and supernatant (S) lanes of the western blots (Figure 17, panels (C) and (D) bottom). Here we expected to see a single band corresponding to RhlE-V5 at 50 kDa. However, two bands were observed in the lysates and supernatants of induced samples (Figure 17, panels (C) and (D) bottom). This may be due to the non-specific binding of anti V5 antibody to a protein other than RhlE.

Highly intense bands appeared in the western blot which were probably corresponding to the byproducts of the antibodies and the protein A. Surprisingly, a band near 50kDa was observed in SDS gels in the product lanes of IRV002 induced with arabinose and IRV002 induced with arabinose and stressed with 60 µM H_2O_2, which did not appear in the western blot (pellet lanes of panel (C) and (D) (top). However, Hfq did not co-immunoprecipitate RhlE.

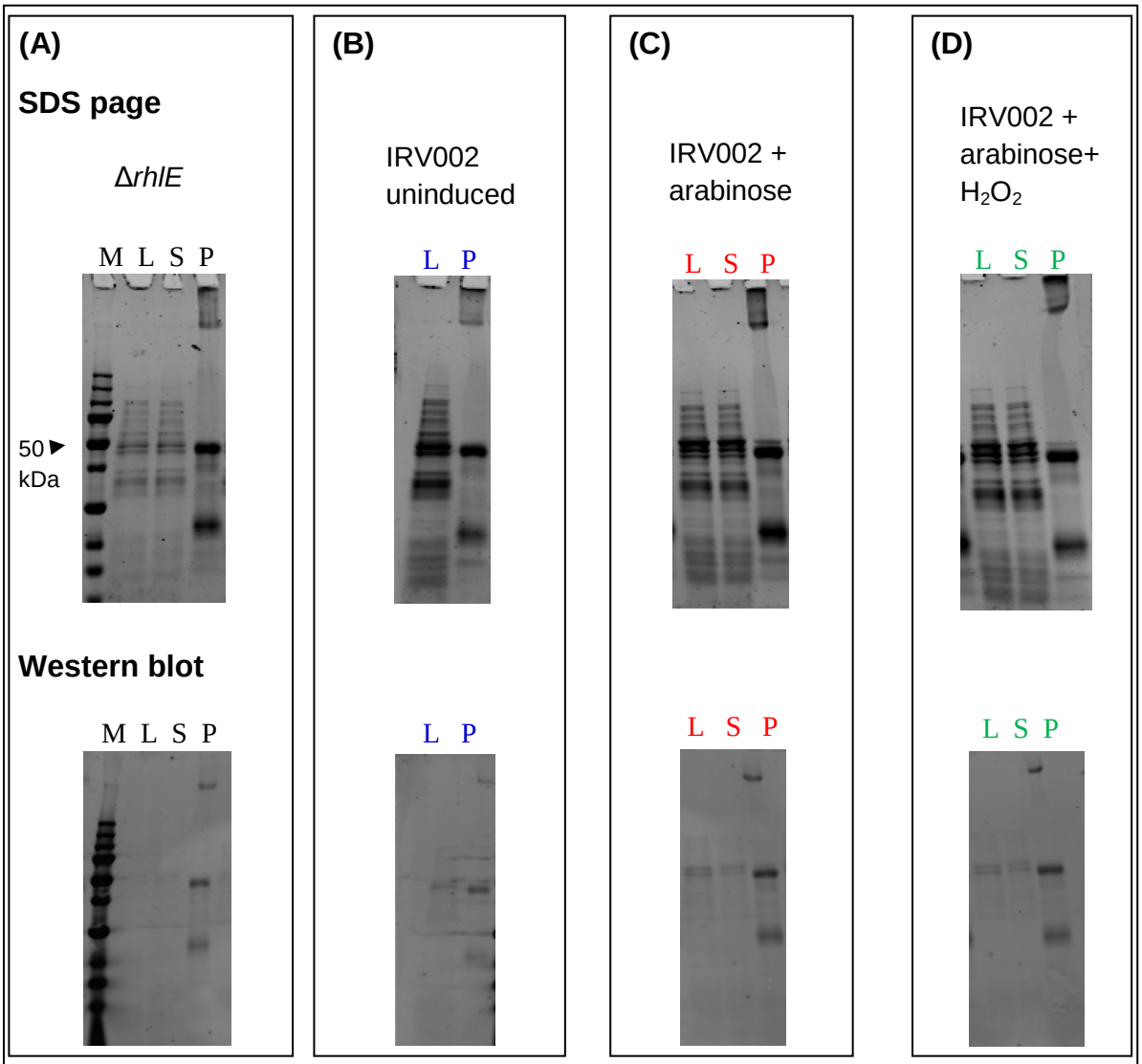

Figure 17: Co-immunoprecipitation of Hfq and RhlE. To investigate whether there is a physical interaction between Hfq and RhlE, *rhlE* gene was amplified with a reverse primer that carries sequence for v5 epitope and was cloned into pBAD24 under arabinose inducible promoter and expressed in Δ*rhlE*. Lysates of Δ*rhlE*, IRV 002 uninduced, IRV 002 induced with 0.01% arabinose and IRV 002 induced with 0.01% arabinose and 60µM H_2O_2 were analyzed. To pull out Hfq-protein complexes anti-Hfq antibody was used and to detect RhlE anti-V5 antibody was used. Top- SDS gel. Bottom- Western blots. L-Lysate, S-Supernatant, P-pellet and M-Marker. (A) Δ*rhlE,* (B) uninduced IRV 002, (C) IRV 002 induced with 0.01% arabinose, (D) IRV 002 induced with 0.01% arabinose and 60µM H_2O_2.

DEAD-box helicases recruit protein partners through their N-terminal or C terminal extensions (47,52). To test whether the C-terminal V5 tag has any effect, co-immunoprecipitation experiments were performed with N-terminal His-tagged RhlE. To pull out Hfq-protein complexes anti-Hfq antibodies were used and anti-His antibodies were used for detection of RhlE-His. No interaction between the two proteins was seen (Data not shown).

CHAPTER FOUR

DISCUSSION

In an attempt to characterize the role of RhlE and Hfq on sRNA-mediated gene regulation, *ΔrhlE* and *ΔrhlE/Δhfq* strains were successfully constructed and examined under different stress conditions. One of the major findings in this study is that *ΔrhlE/Δhfq* shows a recovery in the growth compared to that of the *Δhfq* in the presence of hydrogen peroxide, suggesting a potential role for RhlE under oxidative stress. Defense mechanisms against peroxide-induced oxidative damage partially rely on OxyS-dependent gene regulatory pathways. OxyS base pairing to *fhlA* inhibits the translation of the activator FhlA allowing the organism to recover from oxidative stress (18). In support of the above suggestion that RhlE may play a role in Hfq-dependent OxyS-mediated gene regulation, the present study identified *fhlA* and OxyS as substrates for RhlE. The observation that *fhlA220* stimulates ATPase activity of RhlE by 25-fold relative to RhlE alone can be explained by the recent finding that *fhlA220* is a highly structured RNA (Figure 18) (29). It has been found that some DEAD-box helicases load directly on the double stranded regions of RNAs with the aid of neighboring single stranded regions (49,50). Having many short double-stranded regions separated by single stranded loop structures, *fhlA220* has high potential to stimulate RhlE. Furthermore, at a given time, it may be targeted by more than one RhlE, which can lead to a rapid rate of ATP consumption. Thus, RhlE may be involved in

unwinding of duplex regions of *fhlA220* in order to make structural changes in the overall structure.

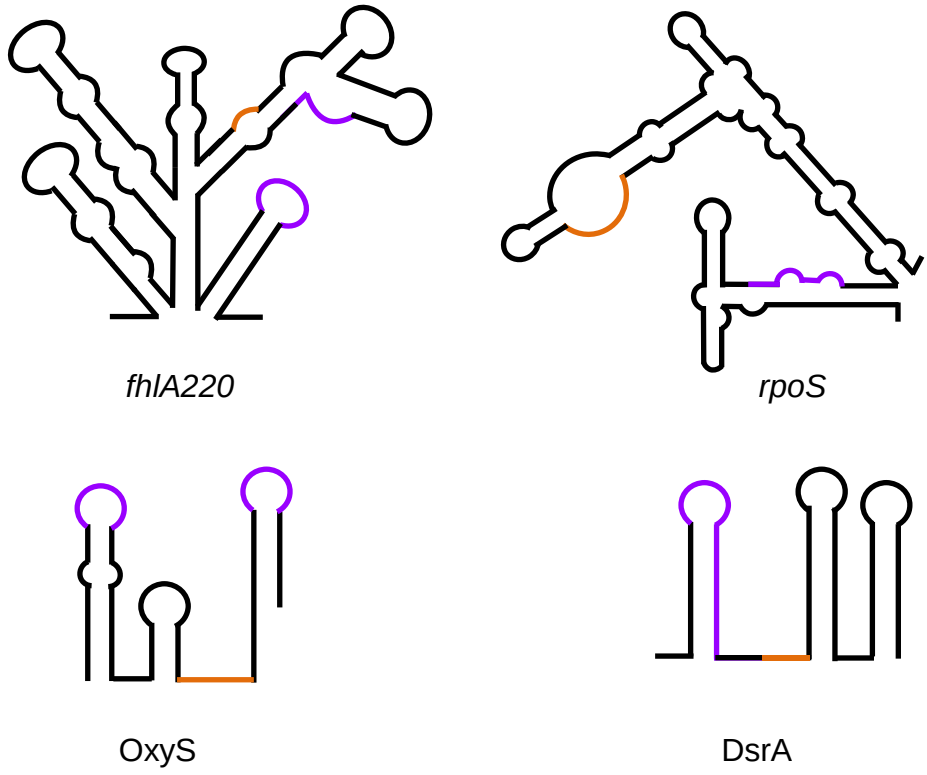

Figure 18: Schematic representation of RNA structures relevant for the present study. RNA structures are drawn from 5' end to 3' end. Hfq binding regions are colored in orange. OxyS base pairs with *fhlA* (28,34,59) and DsrA base pairs with *rpoS* (27). The mRNAs are italicised. mRNA-sRNA interaction regions are colored in purple.

Hfq is a homohexameric protein that lacks ATPase activity. Since Hfq is known to be involved in structural rearrangements of mRNAs and sRNAs, it was speculated that Hfq could be coupled with a helicase. A recent paper identified CsdA which is another *E.coli* DEAD-box helicase, as a required factor for Hfq-mediated *rpoS* regulation by DsrA (61). In this paper, Resch et al. put forward the

idea that CsdA unwinds the *rpoS* translational inhibitory structure, allowing Hfq-bound DsrA to pair with *rpoS* leader region to release the ribosome binding site under the cold shock conditions. They also suggest that CsdA may be involved in recycling of Hfq by rearranging the RNP complex. These findings have clear implications on the present study. Since the growth of *ΔrhlE/Δhfq* was sensitive to oxidative stress and *in vitro* findings of *fhlA* and OxyS being substrates of RhlE imply a potential role for RhlE in *E.coli* oxidative stress pathways. Having helicase activity, RhlE may resolve OxyS and *fhlA* secondary structures thus, allowing Hfq to facilitate base-paring of two RNAs or it may rearrange the OxyS-Hfq-*fhlA* complex to recycle Hfq. It is also possible that, having an interaction surface for RNaseE, RhlE may direct the OxyS-*fhlA* complex to be degraded by the degradosome. Although the findings in the present study are insufficient to elucidate the exact mechanism of RhlE action in this regulation, it is clear that RhlE has implications in the OxyS-mediated *fhlA* repression.

RhlE was identified as a component in the Hfq-DsrA complex (Lee and Feig unpublished data). DsrA base pairs with *rpoS* and activates the translation of RpoS under the cold shock (29). However, deletion of *rhlE* did not change the growth pattern of wt and *Δhfq* under cold shock. Further DsrA did not stimulate the *in vitro* ATPase activity significantly indicating that it might not be a preferential substrate for RhlE *in vivo*. The observations can be justified with the recent finding that CsdA involves in regulation of DsrA-mediated *rpoS* activation (60). Under these circumstances, RhlE may not have a role at low temperatures;

rather, it may be the helicase partner of Hfq under oxidative and sugar stresses. These findings also imply that *E.coli* DEAD-box helicases may have some degree of specificity for RNAs *in vivo* which may be determined by the sequence or the structure of the RNA substrates. Furthermore, since the cold shock regulatory mechanisms lead to active translation of RpoS, we do not expect RhlE to be involved in this regulation at degradation level. However, the present study did not characterize *rpoS* (which is regulated by DsrA) as a substrate for RhlE. As Figure 18 shows the *rpoS* leader sequence is also a structured RNA which may be a potential substrate for RhlE.

Another interesting finding from this study is that Hfq, at its high concentrations, can act as a stimulator for RhlE activity by accelerating the rate of ATP conversion to ADP. Hfq is an abundant cellular protein that participates in regulatory processes by facilitating sRNA-mRNA paring under stress conditions (11). It was found that all DEAD-box helicases including RhlE show poor enzymatic activities *in vitro* (44). This was explained by the fact that DEAD-box helicases recruit other proteins to gain high processivity *in vivo* (45,56). Therefore, it can be speculated that while enhancing RhlE's enzymatic activity, Hfq may be benefited from this RNA helicase to mediate its regulatory roles. However, co-immunoprecipitation experiments failed to identify a direct interaction between RhlE and Hfq. Possible explanation for this could be that, RhlE and Hfq may interact with each other via its RNA substrates or the interaction may be transient.

Another key observation of this study is that *ΔrhlE/Δhfq* exhibits rescued growth over *Δhfq* under sugar stress induced by α-methyl glucose. *E.coli* overcomes sugar phosphate stress by two mechanisms. First, SgrS base pairs to *ptsG* mRNA that leads to translational repression followed by the degradation of RNAs by RNaseE, which in turn inhibits the synthesis of the glucose transporter, PtsG-IICBGlc allowing the organism to recover from sugar stress (16,37,38). Second, SgrT protein encoded within *sgrS* maintains the sugar phosphate tolerance by a mechanism distinct from SgrS. It is also known that either mechanism is sufficient for the recovery (59). SgrS has been characterized as a highly structured sRNA (15), thus it is essential to resolve the secondary structures prior to the base-paring with *ptsG* mRNA. Because RhlE was identified as a part of the SgrS-Hfq complex and since Hfq is known to interact with the degradosome, we hypothesized that RhlE may have a role in Hfq-directed SgrS-*ptsG* degradation. In our experiments, a recovery of *ΔrhlE/Δhfq* in the presence of α-methyl glucose was observed, indicating that RhlE has a role in maintaining sugar phosphate stress. A two stage inhibition pattern throughout the experiment time course was observed for all four strains (wt, *ΔrhlE, Δhfq* and *ΔrhlE/Δhfq*) which may be a result of a selection process that outcompetes individuals incapable of adaptation. After 12 hours from induction, a recovery of the growth was observed for all four strains. It can be speculated that, by this time the cells have evolved mechanisms to metabolize α-methyl glucose, probably by new enzymes which can remove the methyl group at the anomeric carbon leading α-

methyl glucose enter into the glycolytic pathway. The observed growth patterns imply that bacteria achieve sugar-phosphate tolerance by a more complex mechanism(s), and there may be more than one independent or inter-connected regulatory pathway. Further characterization of the system is required to understand the underlying regulatory mechanism and the role of RhlE in these regulatory events.

In conclusion, the ability of *ΔrhlE/Δhfq* to recover from oxidative stress and the identification of *fhlA* and OxyS as substrates of RhlE suggests that RhlE may have a role in Hfq-sRNA mediated gene regulation under oxidative stress. High concentrations of Hfq accelerated the ATPase activity of RhlE in the presence of *fhlA,* suggesting that Hfq may act as a stimulator for the enzyme. *ΔrhlE/Δhfq* also restored the slow growth of *Δhfq* in the presence of α-methyl glucose, indicating that RhlE and Hfq have a synergistic effect under sugar phosphate stress. However, further characterization of this system was not done in this study. Although RhlE was identified in the DsrA-Hfq complex, the observations that *ΔrhlE/Δhfq* showed a similar growth pattern to that of *Δhfq* at 30^{o}C and DsrA did not stimulate the RhlE ATPase activity demonstrate that RhlE may not have a specific role during DsrA-mediated cold shock responses. In an attempt to identify any possible interaction of RhlE with Hfq, co-immunoprecipitation experiments did not show a physical interaction between the two proteins, indicating that RhlE and Hfq do not directly interact with each other to form a stable protein complex.

In summary, these data show that RhlE has implications in Hfq-dependent sRNA-mediated gene regulation under certain stress conditions. To better determine the effect of RhlE in sRNA-mediated gene regulation, it is important to knock out RhlB, the regular member of DEAD box family helicases found in the *E.coli* degradosome (45). Further *ΔrhlE* and *ΔrhlE/Δhfq* knockout strains along with the sRNA (OxyS and SgrS) deleted strains will provide a better understanding of the role of these proteins on sRNA-dependent pathways. Completion of the project will assign a new set of previously unknown cellular functions for RhlE. Further, understanding these regulatory pathways would contribute to the development of potential antibiotics to eradicate pathogenic bacteria.

REFERENCES

1. Padalon-Brauch, G., Hershberg, R., Elgrably-Weiss, M., Baruch, K., Rosenshine, I., Margalit, H., and Altuvia, S. (2008) *Nucleic Acids Res* **36**, 1913-1927
2. Song, T., Mika, F., Lindmark, B., Liu, Z., Schild, S., Bishop, A., Zhu, J., Camilli, A., Johansson, J., Vogel, J., and Wai, S. N. (2008) *Mol Microbiol* **70**, 100-111
3. Toledo-Arana, A., Repoila, F., and Cossart, P. (2007) *Curr Opin Microbiol* **10**, 182-188
4. Valentin-Hansen, P., Johansen, J., and Rasmussen, A. A. (2007) *Curr Opin Microbiol* **10**, 152-155
5. Novick, R. P., Ross, H. F., Projan, S. J., Kornblum, J., Kreiswirth, B., and Moghazeh, S. (1993) *EMBO J* **12**, 3967-3975
6. Romby, P., Vandenesch, F., and Wagner, E. G. (2006) *Curr Opin Microbiol* **9**, 229-236
7. Lenz, D. H., Miller, M. B., Zhu, J., Kulkarni, R. V., and Bassler, B. L. (2005) *Mol Microbiol* **58**, 1186-1202
8. D'Amico, S., Collins, T., Marx, J. C., Feller, G., and Gerday, C. (2006) *EMBO Rep* **7**, 385-389
9. Moxon, E. R., Rainey, P. B., Nowak, M. A., and Lenski, R. E. (1994) *Curr Biol* **4**, 24-33

10. Ochman, H., and Moran, N. A. (2001) *Science* **292**, 1096-1099

11. Gottesman, S. (2004) *Annu Rev Microbiol* **58**, 303-328

12. Papenfort, K., and Vogel, J. (2009) *Res Microbiol* **160**, 278-287

13. Waters, L. S., and Storz, G. (2009) *Cell* **136**, 615-628

14. Mandal, M., and Breaker, R. R. (2004) *Nat Rev Mol Cell Biol* **5**, 451-463

15. Lioliou, E., Romilly, C., Romby, P., and Fechter, P. (2010) *N Biotechnol* **27**, 222-235

16. Aiba, H. (2007) *Curr Opin Microbiol* **10**, 134-139

17. Vogel, J., and Sharma, C. M. (2005) *Biol Chem* **386**, 1219-1238

18. Altuvia, S., Zhang, A., Argaman, L., Tiwari, A., and Storz, G. (1998) *EMBO J* **17**, 6069-6075

19. Majdalani, N., Cunning, C., Sledjeski, D., Elliott, T., and Gottesman, S. (1998) *Proc Natl Acad Sci U S A* **95**, 12462-12467

20. Moller, T., Franch, T., Hojrup, P., Keene, D. R., Bachinger, H. P., Brennan, R. G., and Valentin-Hansen, P. (2002) *Mol Cell* **9**, 23-30

21. Link, T. M., Valentin-Hansen, P., and Brennan, R. G. (2009) *Proc Natl Acad Sci U S A* **106**, 19292-19297

22. Schumacher, M. A., Pearson, R. F., Moller, T., Valentin-Hansen, P., and Brennan, R. G. (2002) *EMBO J* **21**, 3546-3556

23. Brennan, R. G., and Link, T. M. (2007) *Curr Opin Microbiol* **10**, 125-133

24. Tsui, H. C., Leung, H. C., and Winkler, M. E. (1994) *Mol Microbiol* **13**, 35-49

25. Ansong, C., Yoon, H., Porwollik, S., Mottaz-Brewer, H., Petritis, B. O., Jaitly, N., Adkins, J. N., McClelland, M., Heffron, F., and Smith, R. D. (2009) *PLoS One* **4**, e4809

26. Kulesus, R. R., Diaz-Perez, K., Slechta, E. S., Eto, D. S., and Mulvey, M. A. (2008) *Infect Immun* **76**, 3019-3026

27. Sittka, A., Lucchini, S., Papenfort, K., Sharma, C. M., Rolle, K., Binnewies, T. T., Hinton, J. C., and Vogel, J. (2008) *PLoS Genet* **4**, e1000163

28. Mikulecky, P. J., Kaw, M. K., Brescia, C. C., Takach, J. C., Sledjeski, D. D., and Feig, A. L. (2004) *Nat Struct Mol Biol* **11**, 1206-1214

29. Salim, N. N., and Feig, A. L. (2010) *PLoS One* **5**

30. Zhang, A., Wassarman, K. M., Ortega, J., Steven, A. C., and Storz, G. (2002) *Mol Cell* **9**, 11-22

31. Jordi, B. J., and Higgins, C. F. (2000) *J Biol Chem* **275**, 12123-12128

32. Storz, G., and Imlay, J. A. (1999) *Curr Opin Microbiol* **2**, 188-194

33. Resch, A., Afonyushkin, T., Lombo, T. B., McDowall, K. J., Blasi, U., and Kaberdin, V. R. (2008) *RNA* **14**, 454-459

34. Frohlich, K. S., and Vogel, J. (2009) *Curr Opin Microbiol* **12**, 674-682

35. Soper, T. J., and Woodson, S. A. (2008) *RNA* **14**, 1907-1917

36. Majdalani, N., Vanderpool, C. K., and Gottesman, S. (2005) *Crit Rev Biochem Mol Biol* **40**, 93-113

37. Maki, K., Morita, T., Otaka, H., and Aiba, H. (2010) *Mol Microbiol* **76**, 782-792

38. Vanderpool, C. K. (2007) *Curr Opin Microbiol* **10**, 146-151

39. Morita, T., and Aiba, H. (2007) *Proc Natl Acad Sci U S A* **104**, 20149-20150

40. Carpousis, A. J. (2007) *Annu Rev Microbiol* **61**, 71-87

41. Morita, T., Maki, K., and Aiba, H. (2005) *Genes Dev* **19**, 2176-2186

42. Mohanty, B. K., Maples, V. F., and Kushner, S. R. (2004) *Mol Microbiol* **54**, 905-920

43. Chowdhury, S. M., Shi, L., Yoon, H., Ansong, C., Rommereim, L. M., Norbeck, A. D., Auberry, K. J., Moore, R. J., Adkins, J. N., Heffron, F., and Smith, R. D. (2009) *J Proteome Res* **8**, 1504-1514

44. Deiwick, J., Nikolaus, T., Erdogan, S., and Hensel, M. (1999) *Mol Microbiol* **31**, 1759-1773

45. Bizebard, T., Ferlenghi, I., Iost, I., and Dreyfus, M. (2004) *Biochemistry* **43**, 7857-7866

46. Iost, I., and Dreyfus, M. (2006) *Nucleic Acids Res* **34**, 4189-4197

47. Rocak, S., and Linder, P. (2004) *Nat Rev Mol Cell Biol* **5**, 232-241

48. Enemark, E. J., and Joshua-Tor, L. (2008) *Curr Opin Struct Biol* **18**, 243-257

49. Cordin, O., Banroques, J., Tanner, N. K., and Linder, P. (2006) *Gene* **367**, 17-37

50. Jankowsky, E. (2010) *Trends Biochem Sci*

51. Henn, A., Cao, W., Licciardello, N., Heitkamp, S. E., Hackney, D. D., and De La Cruz, E. M. (2010) *Proc Natl Acad Sci U S A* **107**, 4046-4050

52. Jain, C. (2008) *RNA* **14**, 381-389

53. Awano, N., Xu, C., Ke, H., Inoue, K., Inouye, M., and Phadtare, S. (2007) *J Bacteriol* **189**, 5808-5815

54. Prud'homme-Genereux, A., Beran, R. K., Iost, I., Ramey, C. S., Mackie, G. A., and Simons, R. W. (2004) *Mol Microbiol* **54**, 1409-1421

55. Khemici, V., Toesca, I., Poljak, L., Vanzo, N. F., and Carpousis, A. J. (2004) *Mol Microbiol* **54**, 1422-1430

56. Cartier, G., Lorieux, F., Allemand, F., Dreyfus, M., and Bizebard, T. (2010) *Biochemistry* **49**, 2636-2646

57. Wassarman, K. M. (2002) *Cell* **109**, 141-144

58. Sledjeski, D. D., Whitman, C., and Zhang, A. (2001) *J Bacteriol* **183**, 1997-2005

59. Wadler, C. S., and Vanderpool, C. K. (2007) *Proc Natl Acad Sci U S A* **104**, 20454-20459

60. Argaman, L., and Altuvia, S. (2000) *J Mol Biol* **300**, 1101-1112

61. Resch, A., Vecerek, B., Palavra, K., and Blasi, U. (2010) *RNA Biol* **7**, 96-102

ABSTRACT

THE ROLES OF RHLE AND HFQ IN SRNA-DEPENDENT GENE REGULATION

by

ABEYKOON JAYALATH IRESHA SANDEEPANIE RATHNAYAKE

DECEMBER 2010

Advisor: Dr. Andrew Feig

Major: Chemistry

Degree: Master of Science

Bacteria are adapted to live in diverse environmental conditions. Thus, they show excellent tolerance and response to extreme environmental conditions caused by low or high temperatures, high salinity, reactive oxygen species or high nutrient concentrations. sRNAs have been identified and characterized as cis-acting or trans-acting post-transcriptional regulators in diverse cellular processes including virulence and adaptation to environmental stress (12,13,15,16). Interactions of sRNAs and target mRNAs result in translational repression, translational activation or/and degradation of the target. The majority of regulatory small RNAs found in *E.coli* require the RNA binding protein Hfq to perform their roles in gene regulation (11,13,15,16).

Although Hfq is a central player in sRNA mediated gene regulation, how it facilitates these RNA interactions is yet to be discovered. Several studies have shown that Hfq makes Hfq-RNP complexes to mediate its regulatory roles (11,37,40). Previous work in our lab identified RhlE, as a protein partner in SgrS-

Hfq and DsrA-Hfq RNP complexes. RhlE is an ATP-dependent *E.coli* DEAD-box RNA helicase. In the present study it was hypothesized that Hfq and RhlE have a synergistic effect on sRNA-mediated gene regulation. To address this problem, a series of *in vivo* and *in vitro* experiments was carried out.

The growth curve analysis of wt, *ΔrhlE, Δhfq* and *ΔrhlE/Δhfq* revealed that RhlE has a role in Hfq-dependent sRNA-mediated gene regulation under sugar stress and oxidative stress. It was also found that OxyS sRNA, which is transcribed under oxidative stress, and its target *fhlA* mRNA stimulate the ATPase activity of RhlE. Furthermore, DsrA was unable to stimulate RhlE, suggesting that RhlE may have some degree of specificity for RNAs. Although Hfq was shown to stimulate the RhlE ATPase activity in the presence of *fhlA*, the present study did not identify any physical interaction of the two proteins.

These findings have implications for understanding the mechanisms underlying Hfq-dependent sRNA-mediated gene regulation. Complete understanding on sRNA mediated gene regulation and the protein components that are associated with sRNAs, will allow us to use these regulation processes as potential targets for the successful eradication of pathogenic bacteria.

AUTOBIOGRAPHICAL STATEMENT

ABEYKOON JAYALATH IRESHA SANDEEPANIE RATHNAYAKE

Education

2008-current	M.S student, Department of Chemistry, Wayne State Univesity, Detroit MI 48202. Supervisor: Dr. Andrew Feig
2002-2006	B.Sc. Special Degree in Biochemistry and Molecular Biology. University of Colombo, Sri Lanka.

Work Experience

Teaching Assistant: Wayne State University, 2008- 2010.

Research Assistant: Department of Biochemistry and Molecular Biology, Faculty of Medicine, University of Colombo, Sri Lanka.

Research Assistant: Biochemistry and Molecular biology lab, University of Colombo 2006-2007**.**

Assistant Lecture: Faculty of Science, University of Colombo. 2006-2007.

Vocational training - Molecular Biology Laboratory , Durdan's Hospital. 2006.

Publications

The abstract of the **'**Isolation and characterization of RNase E (*rne*) encoding gene from *Corenebacterium glutamicum'* was published in the book of 'Abstracts'; published by the Chemical Society of University of Colombo. (ISBN 978-955-9021-53-7).

Leaderships

- Treasurer, Sri Lankan Student's Association, Wayne State University, USA
- Student member, Chemical Society, University of Colombo (2004-2006)
- Committee member, Senior Science Society, Visakha Vidyalaya, Sri Lanka
- Student member, Astronomical Club, Visakha Vidyalaya, Sri Lanka